PLOS BIOLOGY

RESEARCH ARTICLE

The enterovirus genome can be translated in an IRES-independent manner that requires the initiation factors eIF2A/eIF2D

Hyejeong Kim[1], David Aponte-Diaz[1], Mohamad S. Sotoudegan[1], Djoshkun Shengjuler[2], Jamie J. Arnold[1], Craig E. Cameron[1]*

1 Department of Microbiology and Immunology, School of Medicine, University of North Carolina, Chapel Hill, North Carolina, United States of America, **2** Batavia Biosciences, Leiden, the Netherlands

* craig.cameron@med.unc.edu

Abstract

RNA recombination in positive-strand RNA viruses is a molecular-genetic process, which permits the greatest evolution of the genome and may be essential to stabilizing the genome from the deleterious consequences of accumulated mutations. Enteroviruses represent a useful system to elucidate the details of this process. On the biochemical level, it is known that RNA recombination is catalyzed by the viral RNA-dependent RNA polymerase using a template-switching mechanism. For this mechanism to function in cells, the recombining genomes must be located in the same subcellular compartment. How a viral genome is trafficked to the site of genome replication and recombination, which is membrane associated and isolated from the cytoplasm, is not known. We hypothesized that genome translation was essential for colocalization of genomes for recombination. We show that complete inactivation of internal ribosome entry site (IRES)-mediated translation of a donor enteroviral genome enhanced recombination instead of impairing it. Recombination did not occur by a nonreplicative mechanism. Rather, sufficient translation of the nonstructural region of the genome occurred to support subsequent steps required for recombination. The noncanonical translation initiation factors, eIF2A and eIF2D, were required for IRES-independent translation. Our results support an eIF2A/eIF2D-dependent mechanism under conditions in which the eIF2-dependent mechanism is inactive. Detection of an IRES-independent mechanism for translation of the enterovirus genome provides an explanation for a variety of debated observations, including nonreplicative recombination and persistence of enteroviral RNA lacking an IRES. The existence of an eIF2A/eIF2D-dependent mechanism in enteroviruses predicts the existence of similar mechanisms in other viruses.

Introduction

RNA recombination is an important driver of evolution in positive-strand RNA viruses [1–3]. Myriad examples exist of the creation of pathogenic viral strains by RNA recombination [4–7]. Indeed, it has been suggested that RNA recombination contributed to the evolution of Severe

Acute Respiratory Syndrome Coronavirus 2 (SARS-CoV-2) and is contributing to creation of the ever-changing repertoire of variants circulating globally [8]. A second epidemiological challenge produced by RNA recombination is the creation of virulent, vaccine-derived polioviruses (PVs) by recombination of live, attenuated vaccine strains with circulating, wild species-C enteroviruses [9]. In spite of the prevalence and importance of RNA recombination in virus evolution, an understanding of the biochemistry and cell biology of this process remains woefully incomplete.

Studies of RNA recombination in the species-C enterovirus, PV, have established the molecular and conceptual framework guiding studies of RNA recombination in other positive-strand RNA viruses [10,11]. Mixing of genetically encoded phenotypes between PV variants occurs rapidly upon coinfection [12]. RNA recombination occurs by a template-switching mechanism in which the viral RNA-dependent RNA polymerase (RdRp) initiates RNA synthesis first on one genome (referred to as the donor template) then switches to a second genome (referred to as the acceptor template) during elongation [10,13]. Transfection of two genomes, each of which individually incapable of producing infectious virus, uses RNA recombination to reconstitute an infectious genome [13]. Systems such as these have shown a direct correlation between genetic errors introduced into the genome and the frequency of recombination, implicating RdRp infidelity as a trigger of recombination [14–16].

The RdRp is sufficient for template switching in vitro [17]. Mutations mapping to RdRp-coding sequence can impair RNA recombination [18,19]. These recombination-defective variants replicate well in cell culture under normal conditions [18,19] but are unable to deal with high mutational loads [18] or replicate well in animals [18,19]. Biophysical experiments revealed the existence of a stalled RdRp with its 3′-end of nascent RNA in a single-stranded form [20]. This state was inextricably linked to RNA recombination using a recombination-defective enzyme, thus identifying a putative recombination intermediate [19]. Formation of a single-stranded 3′-end while replicating the donor genome permits this end to hybridize to the acceptor genome [20]. Nucleotide misincorporation and incorporation of certain nucleotide analogs induces formation of the recombination intermediate, interfering with virus multiplication [19].

All steps of the enterovirus lifecycle, including genome replication, occur in association with virus-induced membranes, which are also thought to be sequestered from the cytoplasm and mechanisms therein capable of sensing viral RNA [21–25]. This circumstance requires genomes undergoing recombination to colocalize to the same site of genome replication, the "genome-replication organelle" (RO). How enteroviral genomes are targeted to an RO is not known. The initial goal of this study was to discover mechanisms governing genome trafficking.

We hypothesized that polyprotein determinants present on the translating ribosome have the capacity to target the translating polysome to the site of genome replication (**Fig 1A**). Once present in the RO, translation would ultimately terminate because factors required for translation initiation would be present in the cytoplasm (**Fig 1B**). These genomes would undergo replication and colocalization of distinct genomes would facilitate template switching and phenotypic mixing (**Fig 1B**). If this hypothesis is correct, then interfering with translation of one of the genomes (**Fig 1C**) would preclude trafficking to the genome-replication organelle and recombination (**Fig 1D**).

The only known mechanism for translation of the enteroviral genome uses the canonical internal ribosome entry site (IRES) present in the 5′-untranslated region (UTR) of the genome [26–30]. When we use the term "IRES" in the absence of a modifier, we are referring to this canonical element. Therefore, genetic inactivation of the IRES should impair recombination. This did not occur. Recombination was stimulated substantially. Some have suggested the existence of a replication-independent mechanism for recombination [31]. However, the corresponding study never investigated the possibility of an IRES-independent mechanism for translation.
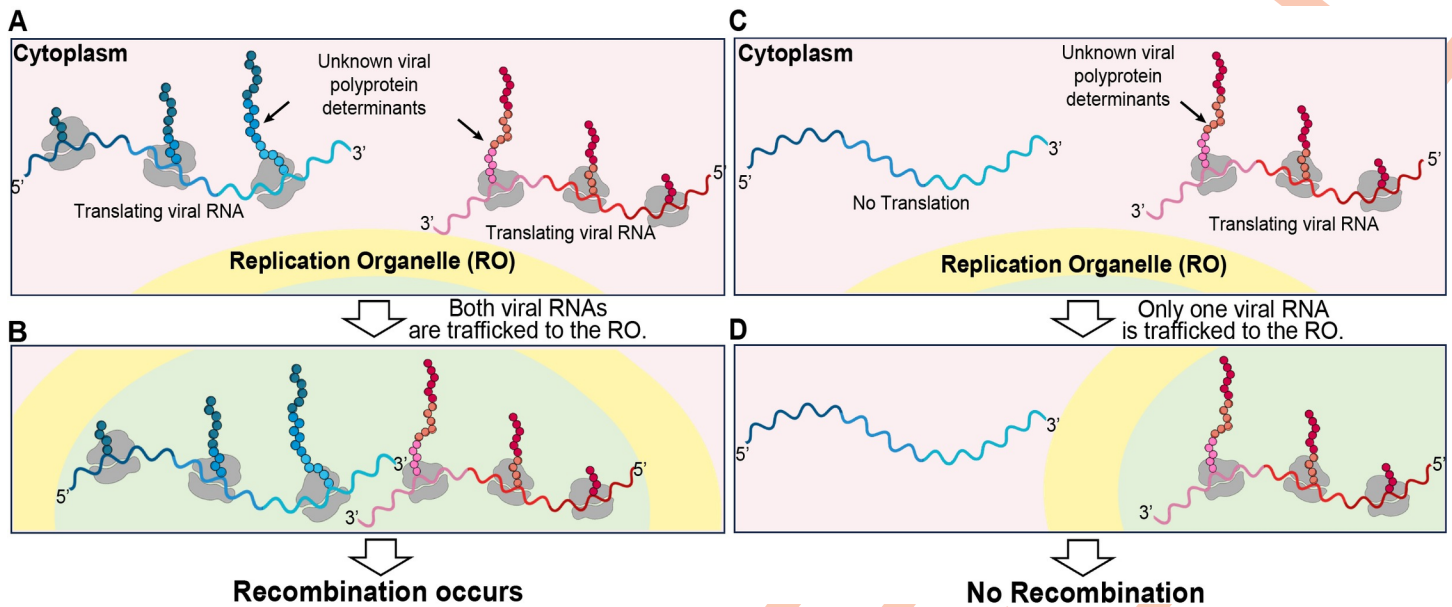
Fig 1. Hypothesis: Polyprotein determinants presented during translation direct the enteroviral genome to the site of replication. For recombination to occur between two genetically distinct PV genomes, these genomes must be in the same replication organelle. **(A, B)** Viral RNAs, shown in blue and red, are targeted to the replication organelle while being translated and facilitate RNA recombination between the two colocalized genomes. Specific viral polyprotein determinants, indicated by a black arrow, mediate this trafficking while still a part of the polyprotein and in association with the ribosome. **(C, D)** In a case where one genome with impaired polyprotein synthesis, shown in red, is also infected by a second genome, shown in blue, the genome with impaired polyprotein synthesis cannot be trafficked to the replication organelle, so recombination between the two genomes cannot occur. This figure was created by Efraín E. Rivera-Serrano using BioRender. PV, poliovirus; RO, replication organelle.

https://doi.org/10.1371/journal.pbio.3001693.g001

Herein, we provide evidence for the existence of a translation–initiation mechanism that requires eIF2A and eIF2D, factors capable of initiating from non-AUG codons [32]. Our data are consistent with initiation occurring at the 3′-end of the 2A protease-coding sequence, downstream of the structural gene (P1) located at the 5′-end of the IRES-dependent open reading frame (ORF). While population-level studies only revealed a role for eIF2A and eIF2D when in vitro transcribed RNA was transfected into cells to initiate infection and/or recombination, studies at the single-cell level suggested a role for these factors during normal, virus-initiated infection.

It is becoming increasingly clear that mechanisms exist for cells to survive under conditions of stress that lead to phosphorylation of eukaryotic translation initiation factor 2α, eIF2α, and shutdown of normal, cap-dependent translation [33]. One of these mechanisms is the use of non-AUG codons for translation initiation using eIF2A and/or eIF2D [34]. Among the earliest responses to viral infection is shutdown of cap-dependent translation by eIF2α kinases [35]. Our study suggests the very provocative possibility that enteroviruses may also exploit the eIF2A/eIF2D-dependent mechanism to survive under conditions in which the cell is actively attempting to thwart viral infection by inhibiting normal translation. Previous attempts to reveal a role for eIF2A and/or eIF2D in multiplication of other viruses may have been masked at the population level [36,37]. Studies at the single-cell level may be necessary to uncover the importance of eIF2A and/or eIF2D in the viral lifecycle.

Results

Evidence for IRES-independent translation of the poliovirus genome

We have used the cell-based assay for PV recombination developed by the Evans laboratory [13]. This assay employs two viral RNA genomes prepared in vitro by T7 transcription of the

appropriate cDNAs [13]. The donor genome is a subgenomic replicon lacking capsid-coding sequence (donor in **Fig 2A**). The acceptor genome is a complete PV genome; however, this genome is replication incompetent because of inactivating mutations within a *cis*-acting replication element (acceptor in **Fig 2A**). Cotransfection of the donor and acceptor genomes into mammalian cells leads to the formation of recombinants capable of producing infectious virus (recombinant in **Fig 2A**). Sufficient virus is produced by this system to permit virus titer to be used as a surrogate for recombination efficiency [13].

We have developed a standardized approach to depict and discuss the recombination experiments performed herein. Donor genomes will be drawn in red and numbered ①, ②, and so on (**Fig 2B**). Acceptor genomes will be drawn in blue, and numbering will pick up from where the donor numbering ended (e.g., ③ in **Fig 2B**). Transfected donor–acceptor pairs will be labeled using the indicated genome numbering (e.g., ① x ③ in **Fig 2C**).

If translation of both donor and acceptor genomes is required for localization within the same genome-replication organelle, then inactivation of translation on one of the genomes should impair recombination. To inactivate translation, we deleted the IRES in the donor template (② in **Fig 2B**) and paired it with the standard acceptor genome (③ in **Fig 2B**). In
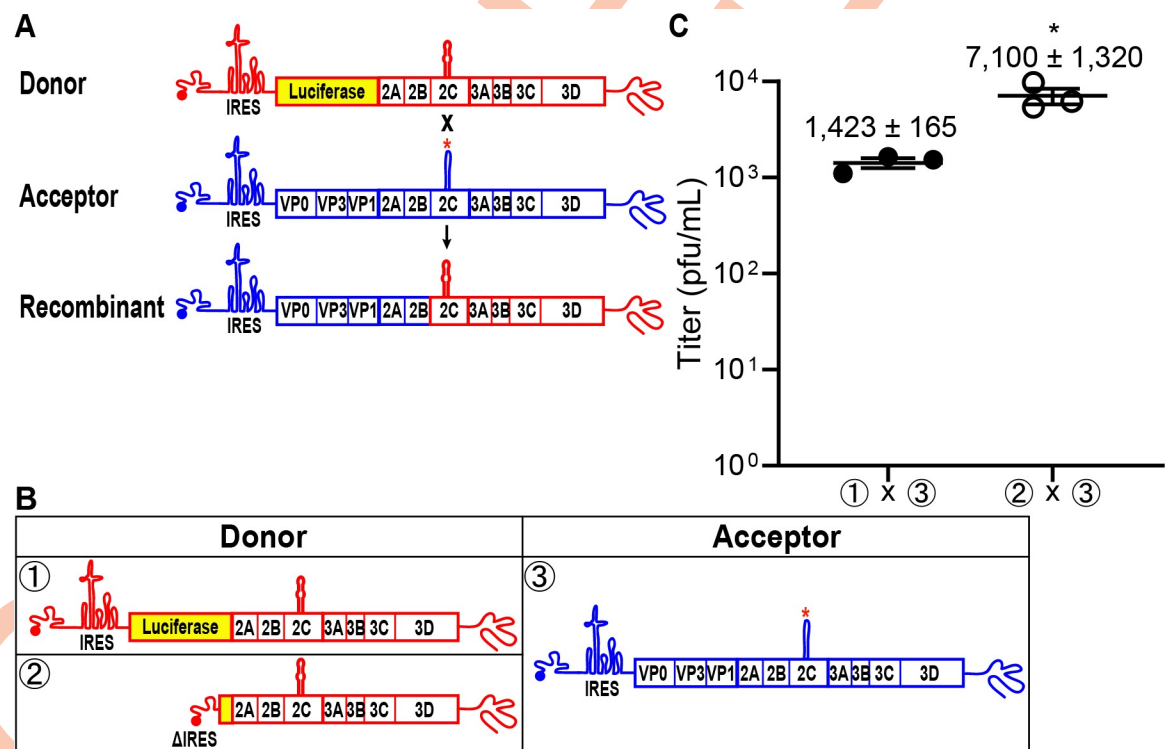
Fig 2. RNA virus recombinants are recovered after deletion of the PV IRES in a donor subgenomic replicon RNA. (A) Schematic of the cell-based assay for PV recombination [13,14,75]. Two RNAs are used in the assay, a replication-competent PV subgenomic RNA (Donor, red) in which capsid-coding sequence is replaced with luciferase coding-sequence and a replication-incompetent full-length PV genomic RNA (Acceptor, blue) with a defective *cis*-acting replication element (indicated by red *). Cotransfection of these RNAs in a L929 mouse fibroblast cell line produces infectious virus if recombination occurs resulting in a replication-competent, full-length PV genomic RNA. Infectious virus produced by recombination can be quantified by plaque assay using HeLa cells. **(B)** Comparison of infectious virus produced between donor RNAs with either an intact IRES (①) or when the entire IRES and majority of luciferase coding sequence (nt 41–2,393, ΔIRES) was deleted (②) [13]. **(C)** Recombination between the donor with the deleted IRES (ΔIRES) and acceptor RNA (② x ③) produces 5-fold more recombinant virus compared to the corresponding control (① x ③). Results show titer of recombinant virus (pfu/mL ± SEM; $n = 3$). Statistical analyses were performed using unpaired, two-tailed t test (* indicates $p < 0.05$). Numerical data provided as Supporting information (S1 Data). IRES, internal ribosome entry site; PV, poliovirus.

https://doi.org/10.1371/journal.pbio.3001693.g002

contrast to expectations, deletion of the IRES enhanced recombination by 5-fold over the control (compare ② x ③ to ① x ③ in **Fig 2C**).

Dogma in picornavirology has been that for a genome to be replicated and, therefore, to serve as a template for recombination, translation of that genome must occur [38,39]. However, it was possible that the polyprotein produced by the acceptor genome might complement the deficit of the donor genome. If this is the case, then eliminating production of the RdRp (3D) by the acceptor genome should inhibit recombination. To test this possibility, we constructed two acceptor genomes. We introduced two stop codons immediately following the 3B-coding sequence, which should eliminate expression of the 3C- and 3D-coding sequence (③ in **Fig 3A**). Because it was unclear if the two stop codons would terminate translation with 100% efficiency, we constructed an acceptor genome that not only contained the two stop codons after 3B but also genetically inactivated the RdRp by mutating the sequence to alter its signature GDD motif to GAA (④ in **Fig 3A**). Pairing the ΔIRES donor genome with either of the acceptor genomes still yielded recombinants (① x ③ and ① x ④ in **Fig 3B**).
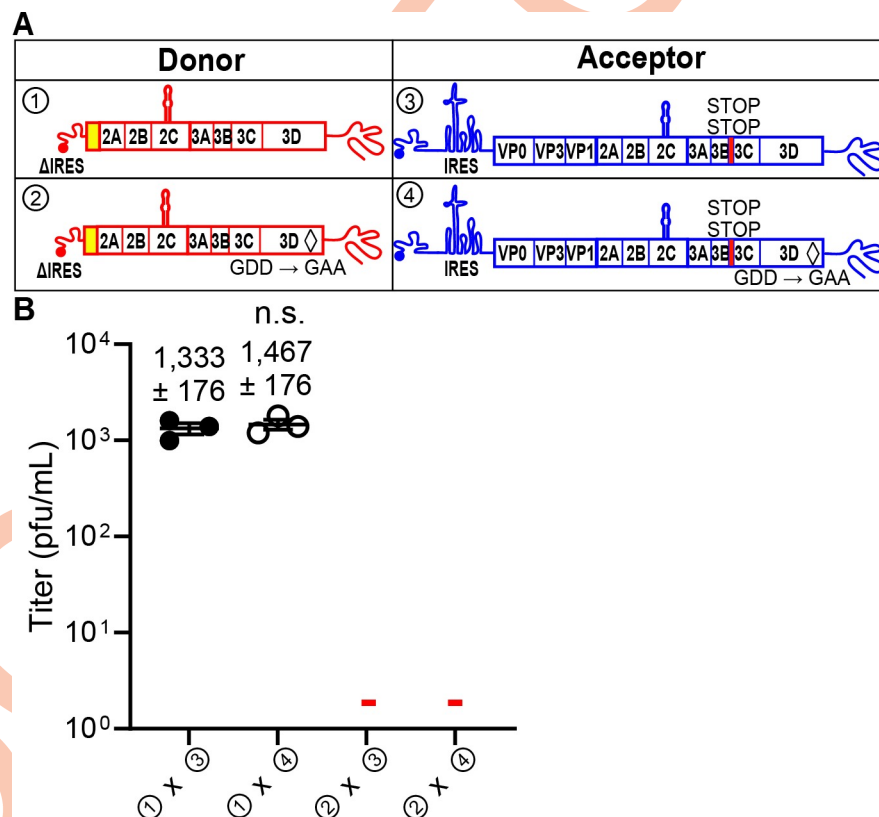
Fig 3. RNA virus recombinants are consistent with the donor RNA as the source of the PV RdRp, 3Dpol, and not the acceptor RNA. (A) A mutation (GDD to GAA) producing an inactive PV RdRp, shown by a black diamond (◊), was introduced into either the donor or acceptor RNAs (② and ④). Insertion of two STOP codons (UAGUAA) after the 3B-coding sequence (3B STOP), indicated by a red rectangle, was introduced into the acceptor RNAs (③ and ④). **(B)** The indicated donor and acceptor RNAs were cotransfected into L929 cells. Yields of recombinant virus following transfection are shown (pfu/mL ± SEM; $n = 3$).—indicates that plaques were not detected (limit of detection: 2 pfu/mL). Statistical analyses were performed using unpaired, two-tailed t test (n.s. indicates not significant). Viral recombinants were recovered only when the donor had an intact 3D gene encoding an active RdRp (① x ③, ① x ④); viral recombinants were not recovered when the donor RNA encoded an inactive RdRp (② x ③, ② x ④). There was no impact on viral recombinants produced when the acceptor RNA had stop codons upstream of the 3D gene encoding an active or inactive RdRp (① x ③, ① x ④). Numerical data provided as Supporting information (S1 Data). PV, poliovirus; RdRp, RNA-dependent RNA polymerase.

https://doi.org/10.1371/journal.pbio.3001693.g003

At this stage, two possibilities remained to explain the observation of recombination using the ΔIRES donor genome. The first possibility was recombination by a nonreplicative, RdRp-independent mechanism, and such a mechanism has been proposed to exist for enteroviruses [31]. However, the second possibility is the existence of an IRES-independent mechanism for translation of the PV genome. If this latter possibility were correct, then it would explain the observations that led to the existence of nonreplicative recombination. By definition, a nonre-plicative mechanism should not require the RdRp. So, we constructed a ΔIRES donor genome that also harbored a genetically inactive RdRp (② in **Fig 3A**). An inactive RdRp would be expected to only interfere with replicative recombination. Pairing the ΔIRES, inactive-RdRp donor genome with either of the acceptor genomes designed to preclude expression of the RdRp abrogated recombination (② x ③ and ② x ④ in **Fig 3B**).

It now appeared that the donor genome was being translated. However, deleting the IRES creates a 5′-end essentially lacking a UTR. In this case, translation initiation might be an irrelevant mechanism. To probe this possibility, we inhibited IRES-dependent translation by deleting 10 nucleotides from stem-loop II-3 (ΔSLII-3) in the donor genomes with or without an active RdRp; these constructs contained the entire luciferase-coding sequence (**Fig 4A**) [40]. We paired each of the ΔSLII-3 donor genomes with each of the acceptor genomes designed to
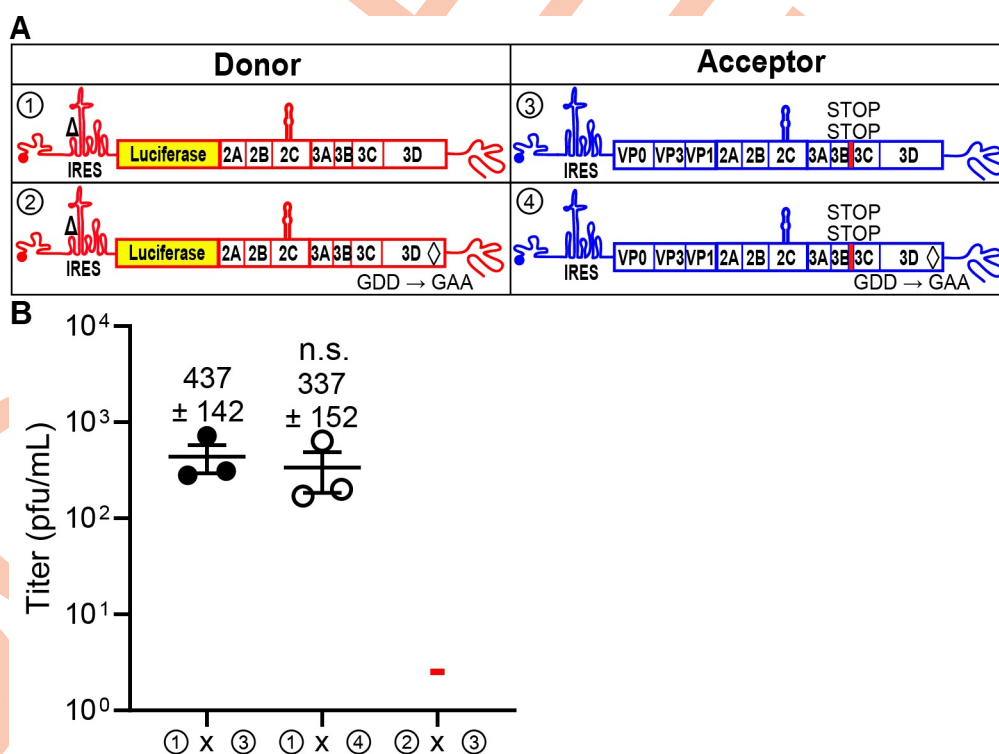
Fig 4. A 10-nt deletion in the IRES that is known to prevent translation recapitulates phenotypes observed with a deleted IRES. (A) The donor RNA was engineered to contain a 10-nucleotide deletion (nt 185–189, nt 198–202) known to disrupt the IRES (referred to as ΔSLII-3) [40] with an active or an inactive RdRp. **(B)** Comparison of infectious virus produced between the indicated donor and acceptor RNAs with the specific modifications. Results show titer of recombinant virus (pfu/mL ± SEM; n = 3).—indicates that plaques were not detected (limit of detection: 2 pfu/mL). Statistical analyses were performed using unpaired, two-tailed t test (n.s. indicates not significant). Viral recombinants were recovered using a donor RNA containing the ΔSLII-3 and an active RdRp with the indicated acceptor RNAs (① x ③, ① x ④); viral recombinants were not recovered when the donor RNA contained ΔSLII-3 and encoded an inactive RdRp (② x ③). Numerical data provided as Supporting information (S1 Data). IRES, internal ribosome entry site; RdRp, RNA-dependent RNA polymerase.

https://doi.org/10.1371/journal.pbio.3001693.g004

preclude expression of the RdRp. The outcomes with ΔSLII-3 donor genomes (**Fig 4B**) were identical to those for the comparable ΔIRES donor genomes (**Fig 3B**), consistent with the idea that an IRES-independent mechanism of translation exists for PV.

Evidence for IRES-independent translation of the enterovirus A71 genome

It was important to evaluate this phenomenon of IRES-independent translation using another enterovirus, because conservation across the genus would be expected for a function essential to virus viability or fitness. We had already adapted EV-A71 for evaluation of recombination using the cell-based system [15]. We constructed an EV-A71 ΔIRES donor genome such that luciferase-coding sequence remained intact (**Fig 5A**). Luciferase activity detected from the subgenomic RNA with a functional IRES in the presence of 3 mM guanidine hydrochloride (GuHCl), an inhibitor of enterovirus genome replication, showed accumulation of luciferase activity in cells (**Fig 5A**). However, deletion of the IRES abolished accumulation of luciferase activity (**Fig 5A**). Therefore, IRES-independent translation either produces luciferase at a level below the limit of detection or initiates downstream of luciferase-coding sequence.

We paired the EV-A71 ΔIRES donor genomes encoding an active or inactive RdRp with acceptor genomes incapable of expressing RdRp-coding sequence (**Fig 5B**). As observed for PV (**Fig 3B**), an active RdRp was required in the donor genome to observe recombination (**Fig 5C**). These data are consistent with recombination occurring by a replicative, RdRp-dependent mechanism, with the RdRp being produced by an IRES-independent mechanism.

IRES-independent translation may initiate within the nonstructural protein-coding sequence

Studies above with EV-A71 donor genomes showed absolutely no detectable luciferase activity (**Fig 5A**). We performed similar experiments for the PV genomes containing ΔIRES and deleted for luciferase-coding sequence (**Fig 6A**) or ΔSLII-3 containing the complete luciferase-coding sequence (**Fig 6B**). No detectable luciferase activity was observed for either construct with an inactive IRES (**Fig 6A and 6B**). Indeed, the activity in the absence of a functional IRES was lower than that detected for the corresponding wild-type (WT) donor genomes in the presence of the genome-replication inhibitor, GuHCl (**Fig 6A and 6B**). Surprisingly, the signal was the same even when luciferase-coding sequence was present (compare ΔSLII-3 in **Fig 6B** to ΔIRES in **Fig 6A**). To determine the limit of detection of the luciferase activity assay, we evaluated the activity of a serial dilution of purified luciferase (**Fig 6C**). The limit of detection was 1.26 pg of luciferase, corresponding to 10^7 molecules of luciferase or 1,200 molecules of luciferase per cell (**Fig 6C**). We were unable to achieve a detectable signal by concentrating the sample from ΔSLII-3. Taken together, we conclude that initiation of translation likely occurs downstream of luciferase-coding sequence in nonstructural protein-coding sequence.

Indirect detection of PV 3CD produced by the IRES-independent mechanism

Translation of PV genomes cannot be detected by immunofluorescence in the absence of genome replication [41]. However, the presence of PV 3CD can be detected in the absence of genome replication because of the capacity of this protein to induce biosynthesis of phosphatidylinositol-4-phosphate (PI4P) [41]. In the uninfected or mock-transfected cell, PI4P localizes to the Golgi apparatus (anti-PI4P in the column marked Mock in **Fig 7**). Transfection and replication of WT PV subgenomic replicon RNA leads to induction and redistribution of PI4P (anti-PI4P in the column marked WT in **Fig 7**). In this circumstance, it is also possible to
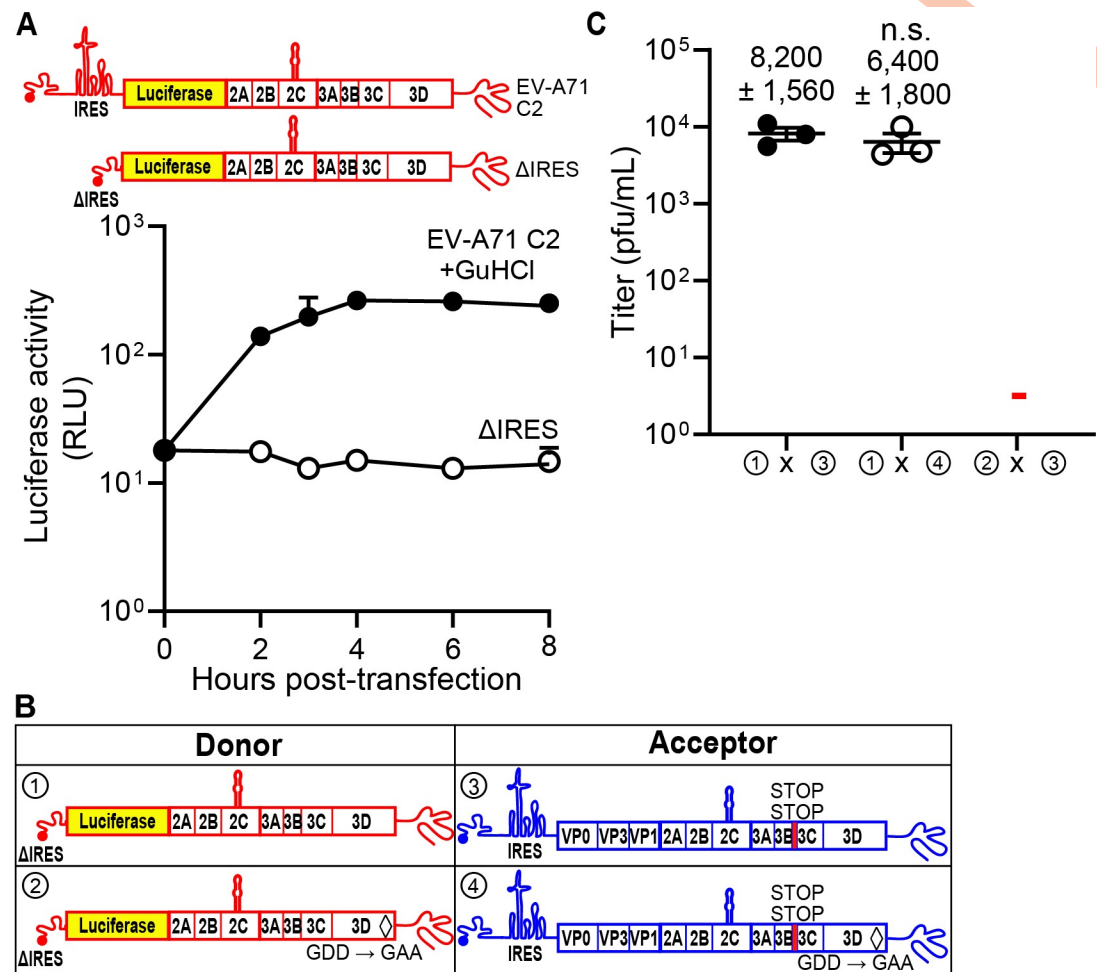
Fig 5. Evidence for IRES-independent translation of the enterovirus A71 genome. (A) Subgenomic replicon luciferase activity using an EV-A71 C2 subgenomic replicon with the entire IRES (nt 38–767) deleted (ΔIRES) [15]. As a control, the WT subgenomic replicon RNA was transfected in the presence of GuHCl, a replication inhibitor. Luciferase activity is reported in RLUs as a function of time posttransfection. Numerical data provided as Supporting information (S1 Data). **(B, C)** Comparison of infectious virus generated between the indicated donor and acceptor RNAs with the specific modifications. The indicated set of donor and acceptor RNAs was cotransfected into RD cells. Results show titer of recombinant virus (pfu/mL ± SEM; *n = 3*).— indicates that plaques were not detected (limit of detection: 2 pfu/mL). Statistical analyses were performed using unpaired, two-tailed *t* test (n.s. indicates not significant). Viral recombinants were recovered only when the donor had an intact 3D gene encoding an active RdRp (① x ③, ① x ④); viral recombinants were not recovered when the donor RNA encoded an inactive RdRp (② x ③). Numerical data provided as Supporting information (S1 Data). GuHCl, guanidine hydrochloride; IRES, internal ribosome entry site; RD, rhabdomyosarcoma; RdRp, RNA-dependent RNA polymerase; RLU, relative light unit; WT, wild type.

https://doi.org/10.1371/journal.pbio.3001693.g005

observe viral proteins (anti-3D in the column marked WT in **Fig 7**). However, PI4P was also induced in the presence of GuHCl (anti-PI4P in the column marked WT + GuHCl in **Fig 7**) [41]. Under these conditions, viral proteins were not detected (anti-3D in the column marked WT + GuHCl in **Fig 7**) [41]. Deletion of the IRES also causes induction of PI4P in the absence (anti-PI4P in the column marked ΔIRES in **Fig 7**) and presence of GuHCl (anti-PI4P in the column marked ΔIRES + GuHCl in **Fig 7**). The same is not true for a full-length genomic RNA containing stop codons following 3B-coding sequence, which would preclude production of 3CD (anti-PI4P in the column marked 3B STOP in **Fig 7**). These observations provide support for the expression of 3CD in the absence of the IRES at levels perhaps on par with those expressed by the WT subgenomic replicon in the presence of GuHCl.
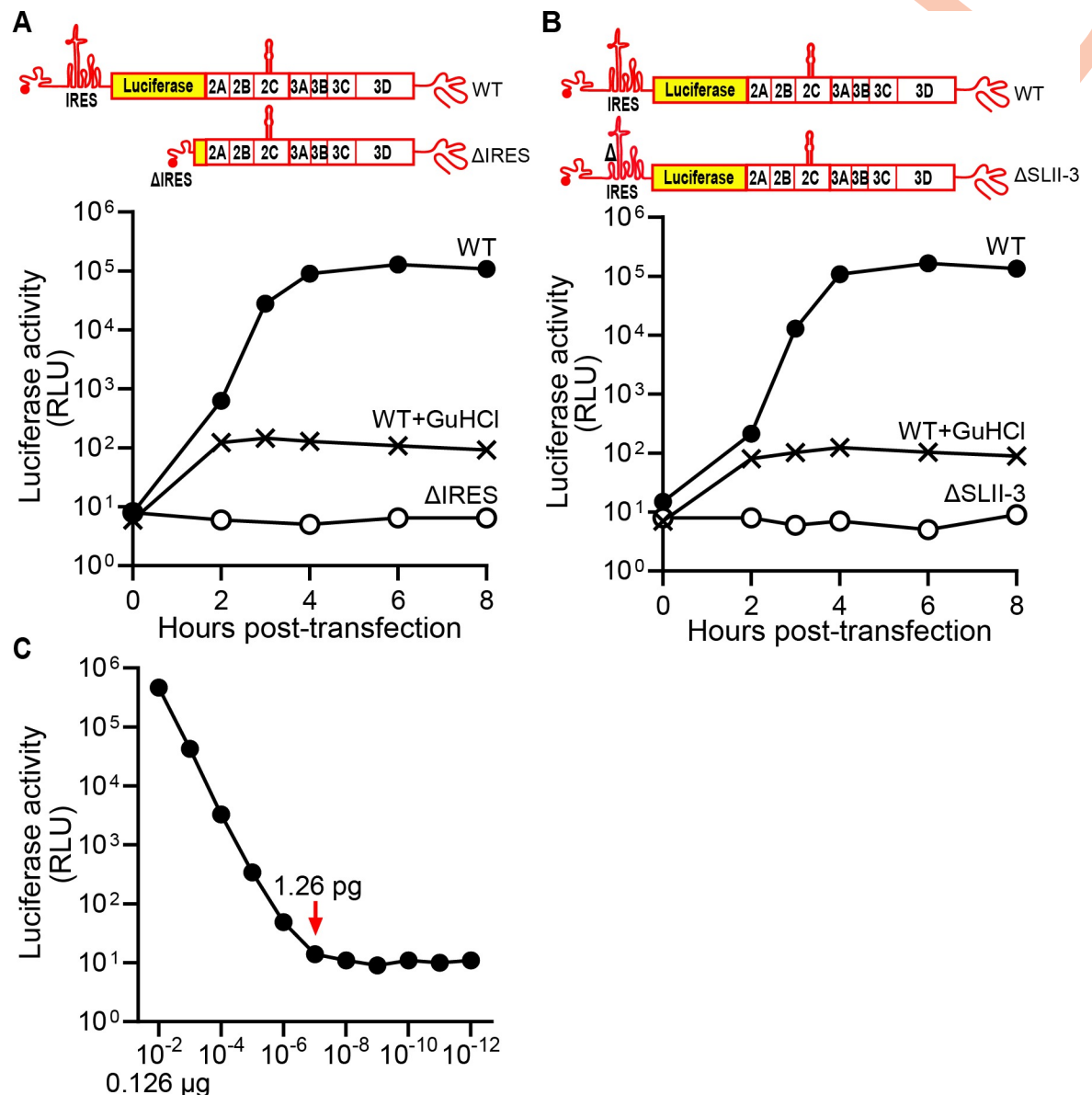
Fig 6. IRES-independent translation may initiate downstream of luciferase-coding sequence within the nonstructural protein-coding sequence. (A, B) Subgenomic replicon luciferase assay comparing the depicted RNAs: WT vs. ΔIRES (panel **A**) and WT vs. ΔSLII-3 RNAs (panel **B**). As a control, the WT RNA was transfected in the presence of GuHCl. Luciferase activity is reported in RLUs as a function of time posttransfection. Luciferase units for ΔIRES and ΔSLII-3 were not detected above 10^1. Numerical data provided as Supporting information (S1 Data). **(C)** Luciferase activity observed for a serial dilution of purified recombinant luciferase enzyme. The initial amount of luciferase in the reaction was 12.6 μg. The limit of detection was reached at a 1×10^7 fold dilution (1.26 pg luciferase), indicated by the red arrow. This corresponds to 1.2×10^7 molecules of luciferase and 1,200 molecules of luciferase per cell from RNAs containing either a deleted IRES or ΔSLII-3. Numerical data provided as Supporting information (S1 Data). GuHCl, guanidine hydrochloride; IRES, internal ribosome entry site; RLU, relative light unit, wild-type.

https://doi.org/10.1371/journal.pbio.3001693.g006

IRES-independent translation occurs in spite of PKR activation and eIF2α phosphorylation

Our experiments use RNA produced by transcription in vitro. The absence of a 5′-cap and the presence of structured RNA at the 5′-end of the viral genome suggest the possibility that the double-stranded RNA-activated protein kinase, PKR, will be activated upon transfection of
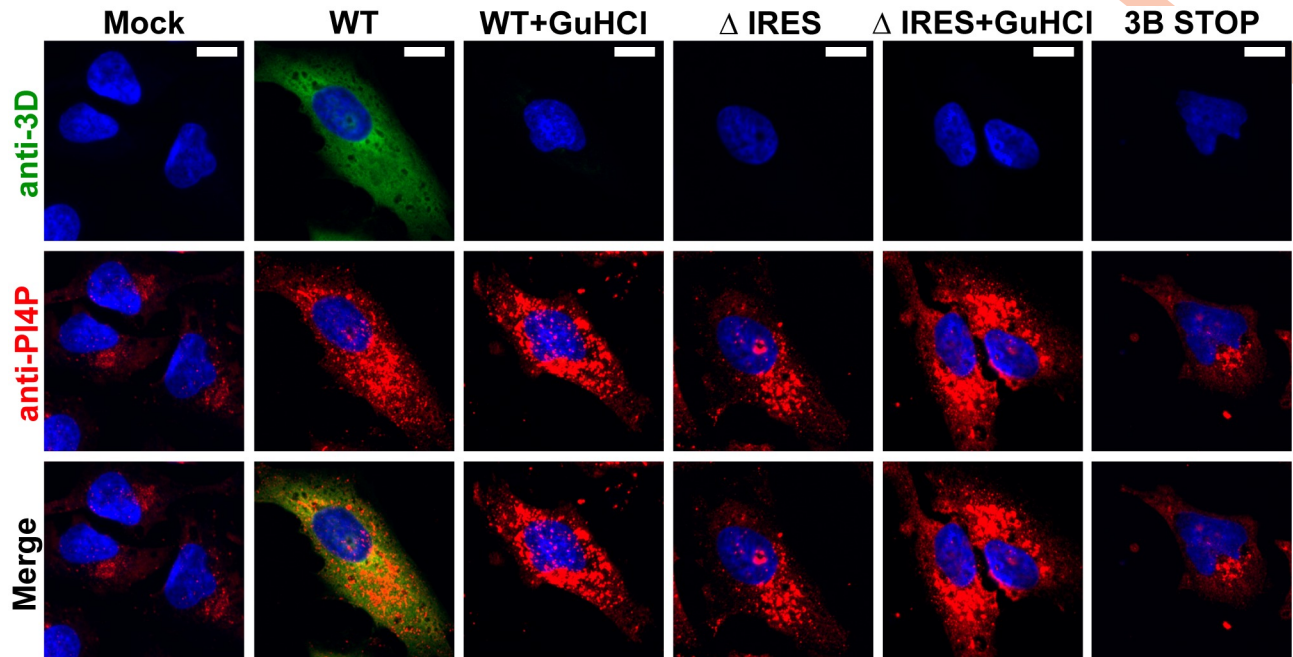
Fig 7. Induction and redistribution of PI4P serve an indirect method to detect production of 3CD by the IRES-independent translation mechanism. Immunofluorescence of cells after transfection. HeLa cells were transfected with in vitro transcribed subgenomic replicon RNAs: WT; ΔIRES, and a full-length genomic RNA with two STOP codons after the 3B-coding sequence: 3B STOP. WT and ΔIRES transfected cells were also treated with 3 mM GuHCl. Six hours posttransfection, cells were immunostained for the presence of PI4P (red) and 3D (green). Nucleus was stained with DAPI (blue). Mock represents cells that were taken through the transfection protocol in the absence of RNA. PI4P was induced and redistributed in cells transfected with WT and ΔIRES, both in the absence and presence of GuHCl, but not 3B STOP. 3D was detected in cells transfected with WT in the absence of GuHCl only. Scale bars are equivalent to 10 μm. GuHCl, guanidine hydrochloride; IRES, internal ribosome entry site; PI4P, phosphatidylinositol-4-phosphate; WT, wild-type.

viral RNA into the cell [42]. Activation of PKR would then lead to phosphorylation of eIF2α and cessation of eIF2-dependent mechanisms of translation initiation in the cell [33].

To assess the status of PKR and eIF2α, we repeated the experiment described above in **Fig 7** and processed the cells for analysis by western blotting. Threonine-446 (T446) phosphorylated PKR was below detectable limits in untransfected cells (mock in **Fig 8A**), but PKR was clearly detectable in these cells (mock in **Fig 8B**). Transfection of all RNAs caused phosphorylation of PKR on T446 (**Fig 8A**). Interestingly, all detectable PKR acquired the hyperphosphorylated state upon transfection of each RNA based on the mobility shift observed (**Fig 8B**). The observed activation of PKR was caused solely by the RNA transfection without any contributions from genome replication as the signals were the same in the presence of a replication inhibitor (WT + GuHCl in **Fig 8A and 8B**). Activation of PKR corresponded to phosphorylation of eIF2α on serine-51 (S51) (**Fig 8C**). We did not observe any changes to the detectable pool of eIF2α (**Fig 8D**). The canonical enterovirus IRES requires eIF2α to function [43]. Therefore, any IRES-independent mechanism used would likely require factors other than eIF2α.

A primary site of initiation of IRES-independent translation is located within 2A-coding sequence

We evaluated the PV nonstructural protein-coding sequence for the presence of methionine residues conserved across members of the enterovirus genus. The first conserved methionine residue was located at the carboxyl terminus of the 2A protease (**Fig 9A**). We reasoned that if
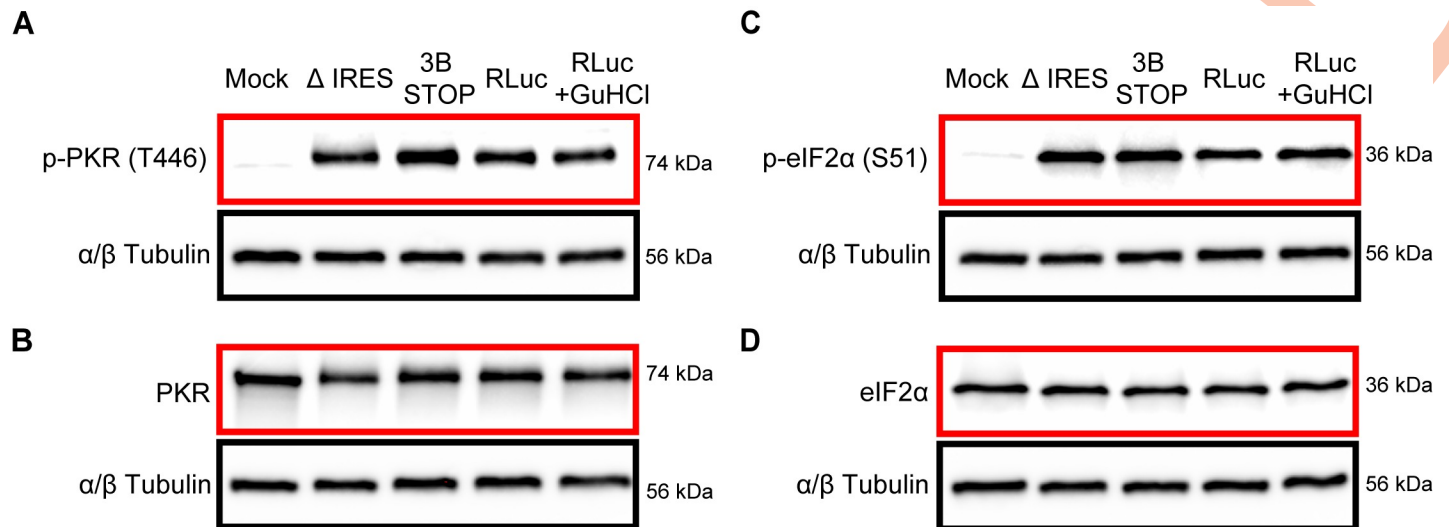
A

B

C

D

Fig 8. Activation of PKR and phosphorylation of eIF2α phosphorylation in response to transfection of PV subgenomic replicon RNA. Western blot analysis of p-PKR (T446) (panel **A**), PKR (panel **B**), p-eIF2α (S51) (panel **C**), and eIF2α (panel **D**) in HeLa cell lysates. Cells were transfected individually with PV subgenomic replicon RNAs: ΔIRES, 3B STOP, and WT or with WT in the presence of 3 mM GuHCl (WT_GuHCl). Six hours posttransfection, cells were processed for western blot analysis and probed using anti-p-PKR (T446), PKR, p-eIF2α (S51), and eIF2α antibodies; α/β tubulin was used as a loading control. Blots provided in Supporting information (S1 Raw Images). GuHCl, guanidine hydrochloride; PKR, RNA-activated protein kinase; PV, poliovirus; T446, threonine-446; WT, wild-type.

https://doi.org/10.1371/journal.pbio.3001693.g008

this methionine residue represented the initiating methionine for the IRES-independent mechanism, then recombination should be inhibited by introducing stop codons downstream of the corresponding AUG in the donor genome, which was observed (② x acceptor in **Fig 9B**). The observed recombination efficiency was reduced by more than 10-fold relative to control (compare to ① x acceptor in **Fig 9B**). Mutation of this AUG codon to UUG or UUU had no effect on recombination (③ or ④ acceptor in **Fig 9B**). However, deletion of this AUG did (⑤ x acceptor in **Fig 9B**). Previous studies of 2A performed by the Wimmer laboratory demonstrated that the carboxyl terminus of 2A was not important for enzyme function, but the nucleotide and/or amino acid sequence in this region was sensitive to mutation [44]. We suggest that the conserved methionine residue is the first residue of the polyprotein produced by the IRES-independent mechanism. However, the sequence of the initiation codon used may not be restricted to AUG codon.

Contribution of eIF2A and eIF2D to IRES-independent translation

Initiation of translation in mammals is no longer thought to be as specific as it once was. Use of non-AUG codons under conditions in which eIF2α is active is now well documented [32,45] (**Fig 10A**). However, under conditions of stress in which eIF2α is phosphorylated and normal translation is no longer active, alternative mechanisms of translation initiation have evolved [32,33]. One such mechanism utilizes eIF2A and eIF2D. In addition to initiating at an AUG codon, these alternative initiation factors use a variety of unique and overlapping codons (**Fig 9A**) [32]. The most direct test of the use of eIF2A and eIF2D is genetic ablation of the expression of one or both. This approach was facilitated by using the HAP1 cell line [46,47]. HAP1 cells are a near-haploid, human cell line derived from the KBM-7 myelogenous leukemia cell line [46]. HAP1 cell lines null for expression of most nonessential genes are available in the Horizon Discovery knockout (KO) collection [48].

HAP1 cells supported the IRES-independent mechanism of translation in the context of the cell-based PV recombination assay (donor ① in **Fig 10B**). As we will describe below, these cells

A

```
                                              → UAGUAA
                                                AAUUAC
PV      120 MGLITAGGEGVVAFADVRDLFAYEEEVMEQ 149 GITNY
EV-A71  121 VGIVSTGGNGLVGFADVRDLLWLDEEAMEQ 150 GVSDY
CVB3    118 IGIVTMGGEGVVGFADIRDLLWLEDDAMEQ 147 GVKDY
EV-D68  118 IGLLTAGGGGIVAFTDIRNLLWLDTDAMEQ 147 GITDY
```

B

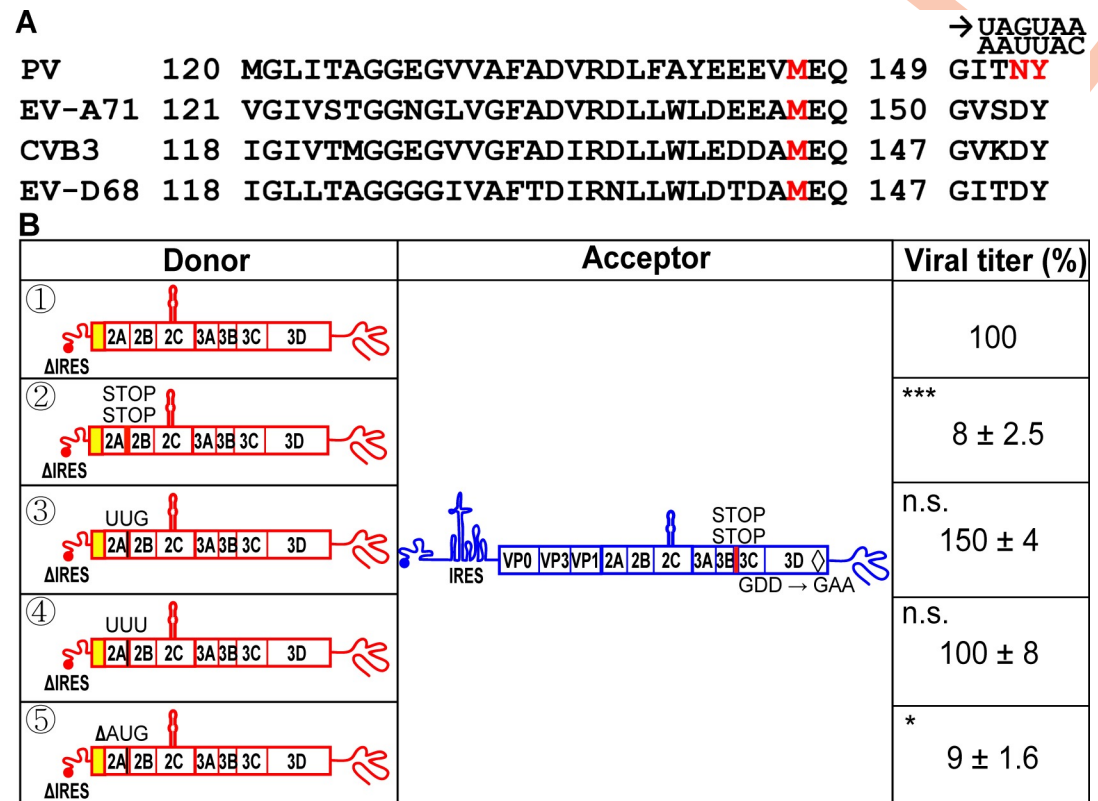| Donor	Acceptor	Viral titer (%)
① ΔIRES		100
② STOP STOP ΔIRES		*** 8 ± 2.5
③ UUG ΔIRES	IRES — VP0 VP3 VP1 2A 2B 2C 3A 3B 3C 3D (STOP STOP / GDD → GAA)	n.s. 150 ± 4
④ UUU ΔIRES		n.s. 100 ± 8
⑤ ΔAUG ΔIRES		* 9 ± 1.6

Fig 9. Deletion of a conserved AUG in the 2A-coding sequence reduces translation of the donor RNA leading to a reduction in viral RNA recombinants. (A) Primary amino acid sequence alignment of a portion of 2A sequence from PV, EV-A71, CVB3, and EV-D68. Numbers refer to 2A protein sequence. The conserved methionine is shown in red. The sites for the insertion of two STOP codons are shown in red; the codons AAU and UAC were changed to UAG and UAA, respectively. **(B)** Comparison of infectious virus produced by the indicated donor RNAs with the specified modifications: ①: ΔIRES; ②: Insertion of two STOP codons after the 2A-coding sequence (2A STOP); ③: AUG to UUG; ④: AUG to UUU; ⑤: ΔAUG. Sites for the modifications are depicted. In all cases, the acceptor RNA contained two STOP codons after 3B-coding sequence (3B STOP) and the mutation that inactivates the RdRp (GDD to GAA). Indicated are the relative viral titers with the average viral titer from recombination using ΔIRES donor (①) and acceptor set as 100% (7,500 pfu/mL, mean ± SEM; $n = 3$). Statistical analyses were performed using unpaired, two-tailed t test (* indicates $p < 0.05$, *** indicates $p < 0.001$, n.s. indicates not significant). The 2A STOP and ΔAUG reduced viral recombinants, while the AUG to UUG and AUG to UUU did not. Numerical data provided as Supporting information (S1 Data). IRES, internal ribosome entry site; PV, poliovirus; RdRp, RNA-dependent RNA polymerase.

also turn out to be susceptible to PV infection. The conserved AUG codon in 2A-coding sequence was required in the HAP1 background (donor ② in **Fig 10B**). Both unique and shared non-AUG codons used for initiation by eIF2A and eIF2D were well tolerated as substitutions for AUG in the donor genome (donors ③, ④, and ⑤ in **Fig 10B**). The eIF2A and/or eIF2D-utilized codons, UUG and CUG, both code for leucine. CUA and CUC codons also code for leucine but are not utilized by either eIF2A or eIF2D (**Fig 10A**) [32]. These two codons were not as well tolerated as the other leucine codons (donors ⑥ and ⑦ in **Fig 10B**). Together, these data are consistent with a role for eIF2A and/or eIF2D in IRES-independent translation.

To probe the role of eIF2A and eIF2D in IRES-independent translation, we evaluated recombination using the ΔIRES donor in eIF2A-KO and eIF2D-KO cell lines (**Fig 10C**). The absence of either factor diminished recombination by nearly 8-fold relative to WT cells (**Fig 10C**). Interestingly, recombination driven by proteins produced by an IRES-dependent mechanism also exhibited a dependence on eIF2A and eIF2D, with recombination reduced by 15-fold in the absence of either factor (**Fig 10D**).
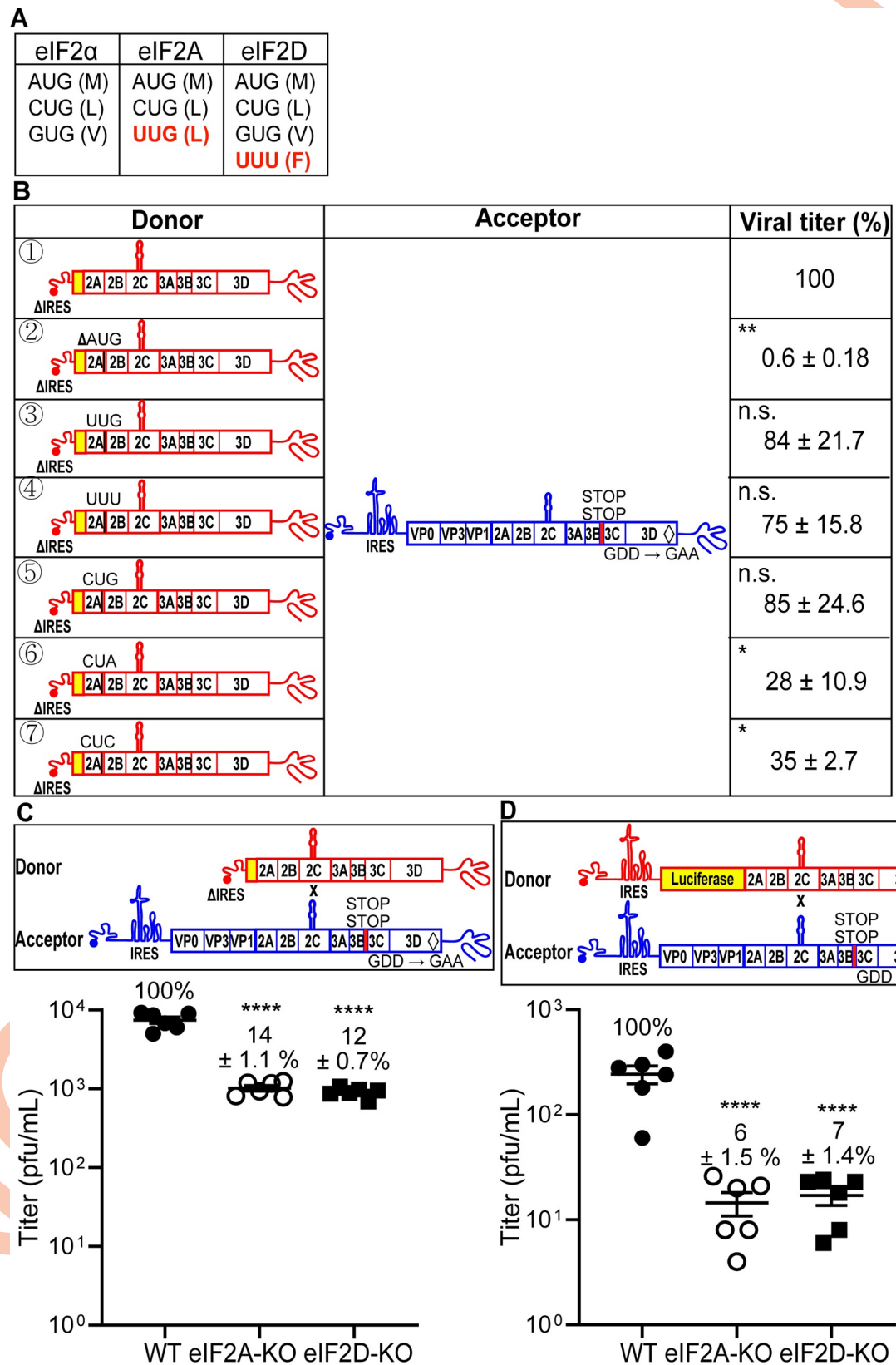
Fig 10. eIF2A and eIF2D initiation factors contribute to IRES-independent translation. (A) Start codons utilized by eIF2, eIF2A, and eIF2D initiation factors [32]. Amino acids for each codon is in parentheses. Initiation factor-specific start codons are indicated in red. **(B)** Comparison of infectious virus produced by the indicated donor RNAs with modifications that alter the conserved AUG to initiation factor specific start codons: ①: ΔIRES; ②: ΔAUG; ③: AUG to UUG; ④: AUG to UUU; ⑤: AUG to CUG; ⑥: AUG to CUA; ⑦: AUG to CUC. Codons UUG, UUU, and CUG can be utilized by initiation factors, but CUA and CUC cannot. In all cases, the acceptor RNA contained two STOP codons after 3B-coding sequence (3B STOP) and the mutation that inactivates the RdRp (GDD to GAA). The indicated set of donor and acceptor RNAs in a 1:5 molar ratio (total 0.3 μg) was cotransfected into HAP1 WT cells. Indicated are the relative viral titers with the average viral titer from recombination using ΔIRES donor (①) and acceptor set as 100% (647 pfu/mL, mean ± SEM; n = 3). Statistical analyses were performed using unpaired, two-tailed t test (*significance level p = < 0.05, ** p = < 0.01, n.s. indicates not significant). The ΔAUG, CUA, and CUC reduced viral recombinants significantly, while UUG, UUU, and CUG did not, consistent with eIF2A and eIF2D contributing to IRES-independent translation. Numerical data provided as Supporting information (S1 Data). **(C, D)** Viral recombinants are reduced in HAP1 cells deficient for eIF2A and eIF2D expression. The indicated set of donor and acceptor RNAs was cotransfected into HAP1 WT or eIF2A-KO or eIF2D-KO cells. Donor RNA: ΔIRES (panel **C**); RLuc-WT (panel **D**). Relative viral titers with the average viral titer from HAP1 WT set as 100% were shown (panel **C**, 7,433 pfu/mL; panel **D**, 243 pfu/mL; mean ± SEM). Statistical analyses were performed using unpaired, two-tailed t test (**** indicates $p < 0.0001$). Numerical data provided as Supporting information (S1 Data). IRES, internal ribosome entry site; KO, knockout; RdRp, RNA-dependent RNA polymerase; WT, wild-type.

https://doi.org/10.1371/journal.pbio.3001693.g010

Evidence for a *cis*-acting RNA element required for eIF2A/eIF2D-dependent translation initiation

As a part of a published study on triggers and mechanisms of template switching by enteroviral polymerases, we completed an RNA sequencing experiment for EV-A71 (data deposited in the Gene Expression Omnibus (GEO) repository under accession number GSE183959) [19]. We used that data set to analyze the nucleotide-substitution frequency across the genome (**Fig 11A**). We identified a 78-nt stretch upstream of the AUG used for eIF2A/eiF2D-dependent, translation–initiation mechanism as a site with a below average frequency of mutation (**Fig 11B**). Both the nucleotide and amino acid sequences in this region for prototype species in the enterovirus genus exhibited a moderate (black asterisks indicate complete conservation) to high (red asterisks indicate conservation in three of the four enteroviruses) sequence conservation, depending on the constraints applied (**Fig 11C**). This 78-nt sequence folded into an RNA structure for all enteroviruses, although the details differed more substantially than expected for sequence conservation (**Fig 11D**). Further empirical analysis of this region will be required to elucidate the bona fide structure.

To assess the functional significance, if any, of this 78-nt stretch of RNA, we evaluated the impact of deleting this sequence on the efficiency of PV RNA recombination. Deletion of the 78-nt sequence (Δ78) in the donor RNA caused a significant reduction in recombination (see ② X acceptor in **Fig 11E**). Substituting the PV sequence with that from EV-A71 or EV-D68 was worse than deleting the sequence (see ③, ④ X acceptor in **Fig 11E**).

Because recombinant viruses produced by these donor–acceptor pairs would reconstitute the WT, PV 78-nt sequence, impaired virus production likely reflects impaired translation caused by introducing the 78-nt sequence from other viruses. We evaluated the ability of the various constructs to support translation using the PI4P-induction assay (**Fig 11F**). The Δ78 construct was as defective for PI4P induction as the ΔAUG construct (**Fig 11F**). The simplest interpretation of this experiment is that the 78-nt sequence represents a *cis*-acting RNA element required for eIF2A/eIF2D-dependent translation. The introduction of the sequences from EV-A71 or EV-D68 did not cause a significant change in PI4P induction (**Fig 11F**). The lack of congruence between this assay and the recombination assay above may reflect a much lower requirement in translation to induce PI4P relative to that required to produce recombinant virus. Future experiments will need to be performed to distinguish between these possibilities.
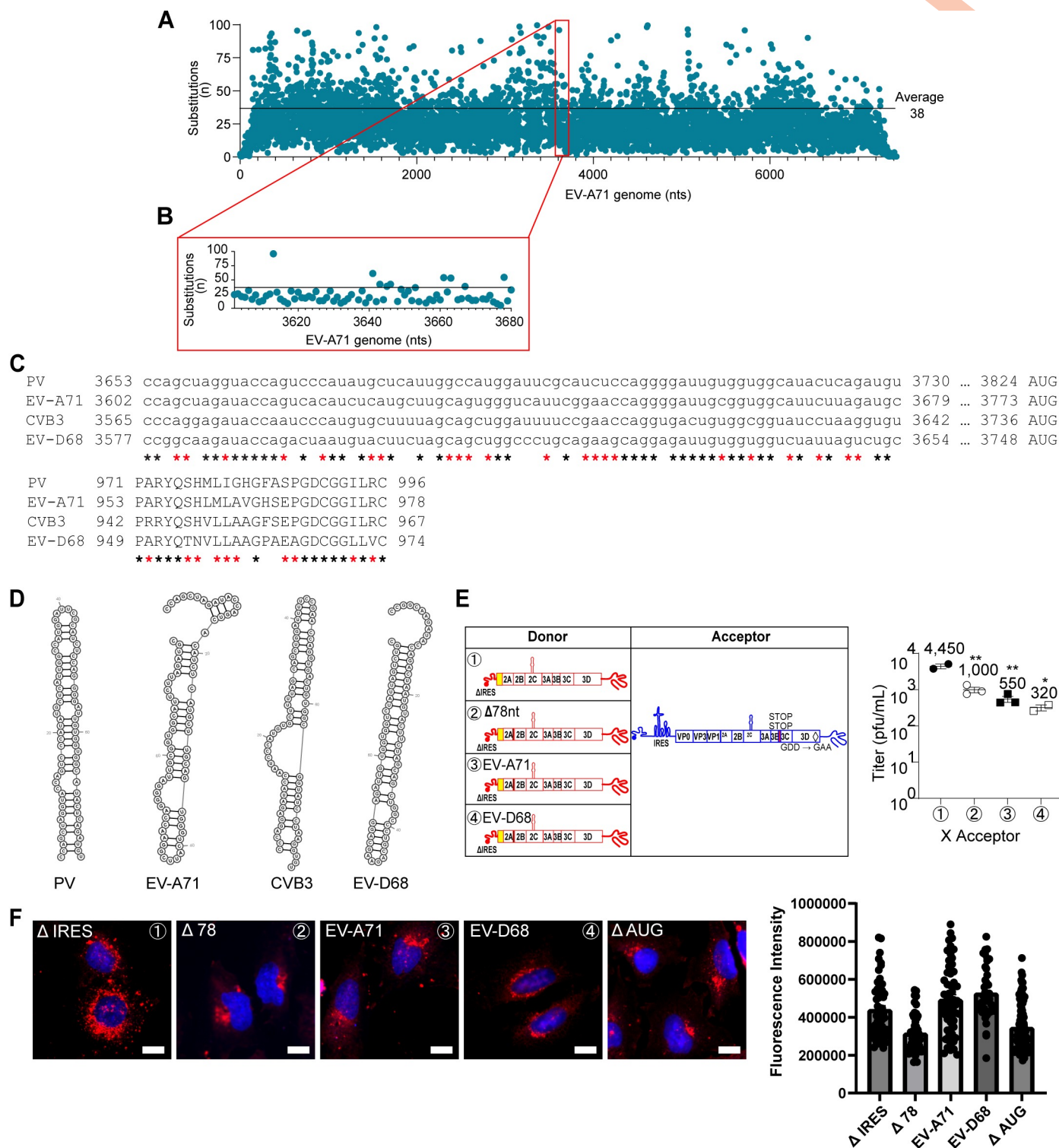
Fig 11. Identification of an RNA sequence upstream of the AUG codon required for eIF2A/2D-dependent translation. (A) Nucleotide substitutions at each position across the EV-A71 genome have been defined by deep RNA sequencing. The average substitution frequency is 38. Some regions exhibit a lower average; these regions of the genome may encode *cis*-acting RNA elements. Numerical data provided as Supporting information (S1 Data). The entire data set is available at the GEO repository under accession number GSE183959. **(B)** The region from 3,602–3,679 of the EV-A71 genome exhibits a below-average frequency of nucleotide substitutions. This region corresponds to a sequence 78-nt upstream of the AUG used for eIF2A/2D-dependent translation. Numerical data provided as Supporting information (S1 Data). **(C)** Alignment of the corresponding nucleotide sequence and amino acid sequence reveals moderate to high sequence identity among enterovirus (PV, EV-A71, CVB3, and EV-D68). Black asterisks indicate conservation across all enteroviruses; red asterisks indicate conservation in three of the four

enteroviruses. **(D)** RNA secondary structure is predicted in this region for all enteroviruses. The RNAfold algorithm was used. The details of the fold varied across the enteroviruses more substantially than sequence might predict. **(E)** Comparison of infectious PV produced using donor RNAs harboring a deletion of the 78-nt sequence (Δ78 nt) or containing the corresponding sequences from EV-A71 or EV-D68. The acceptor RNA used does not support translation of 3CD or an active polymerase. Virus produced (pfu/mL ± SEM; n = 3) from each cotransfection is shown. Statistical analyses were performed using unpaired, two-tailed t test (* indicates $p < 0.05$, ** indicates $p < 0.01$; n.s. indicates nonsignificant). The sequence contributes to production of virus. Numerical data provided as Supporting information (S1 Data). **(F)** Contribution of the 78-nt sequence to IRES-independent translation indirectly by monitoring PI4P levels and localization as described in the legend to **Fig 7**. Donor RNAs of panel E were used, in addition to the ΔAUG donor RNA used in **Fig 9** that has a strong defect to virus production. Quantitation of PI4P staining in approximately 60 cells selected randomly from three separate fields expressed as fluorescence intensity is shown. A significant reduction of PI4P/ translation of the genome ($p < 0.0001$) was observed for Δ78 and ΔAUG only. Scale bars are equivalent to 10 μm. Numerical data provided as Supporting information (S1 Data). GEO, Gene Expression Omnibus; IRES, internal ribosome entry site; PI4P, phosphatidylinositol-4-phosphate; PV, poliovirus.

https://doi.org/10.1371/journal.pbio.3001693.g011

Launching genome replication by infection suppresses the requirement for eIF2A and/or eIF2D

As shown above, launching genome replication by RNA transfection leads to activation of PKR [42] and perhaps other pattern recognition receptors (PRRs) contributing to innate immunity [49]. Activation of PKR would lead to phosphorylation of eIF2α and the need for eIF2A or eIF2D. However, infection might not exhibit the same dependence on these alternative translation initiation factors because the 5′-VPg may preclude activation of PKR and other PRRs.

As a part of our effort to detect IRES-independent translation by monitoring the activity of an expressed reporter, we constructed a genomic replicon harboring nanoLuciferase (NL, Nluc, or nanoLuc) between 2C- and 3A-coding sequences. Surprisingly, this construct actually replicated, yielding a 4-log amplification of nanoLuc activity, and GuHCl inhibited replication (**Fig 12A**). This tool permitted us to compare outcomes for transfection or infection in the absence or presence of eIF2A or eIF2D. As observed for the traditional luciferase reporter (**Fig 10D**), replication of this nanoLuc replicon benefited substantially from the presence of eIF2A and eIF2D when RNA was introduced by transfection (**Fig 12B**). In contrast, introduction of the nanoLuc reporter by infection did not exhibit a significant dependence of either eIF2A or eIF2D (**Fig 12C**). Simultaneous elimination of both eIF2A and eIF2D exhibited a phenotype equivalent to that observed for the individual KOs (**Fig 12D**). We validated the HAP1 KO cell lines used by evaluating expression of eIF2A and eIF2D using western blotting (**Fig 12E and 12F**). Importantly loss of eIF2A or eIF2D did not impact the level of eIF2α in cells (**Fig 12G**). We were unable to perform the comparable experiments with EV-A71 because this virus does not replicate well or spread in the HAP1 background. We conclude that an IRES-independent, eIF2A/eIF2D-dependent mechanism exists in PV and other enteroviruses to sustain replication under conditions in which the "normal" mechanism for translation initiation is unavailable.

Single-cell analysis suggests a role for eIF2A and eIF2D during infection

It is becoming increasingly clear that analysis of viral replication dynamics at the population level can mask phenotypes [50]. For these experiments, we use a GFP reporter expressed by infectious PV to monitor replication dynamics in 100 to 200 single cells at intervals of 30 minutes for 12 to 24 hours [50,51]. We evaluate four parameters: (1) start point, which is the time in which the fluorescence becomes detectable and indicates an infection has been established; (2) maximum, which is the maximum value of the observed fluorescence and correlates with the magnitude of genome replication; (3) slope, which is the rate of the fluorescence change and correlates with the speed of genome amplification; and (4) infection time, which is the time from start to maximum and correlates with the virus generation time [50]. We plot distributions of these parameters and perform statistical tests to determine if the perturbation under investigation causes a significant difference relative to the control [50,51].
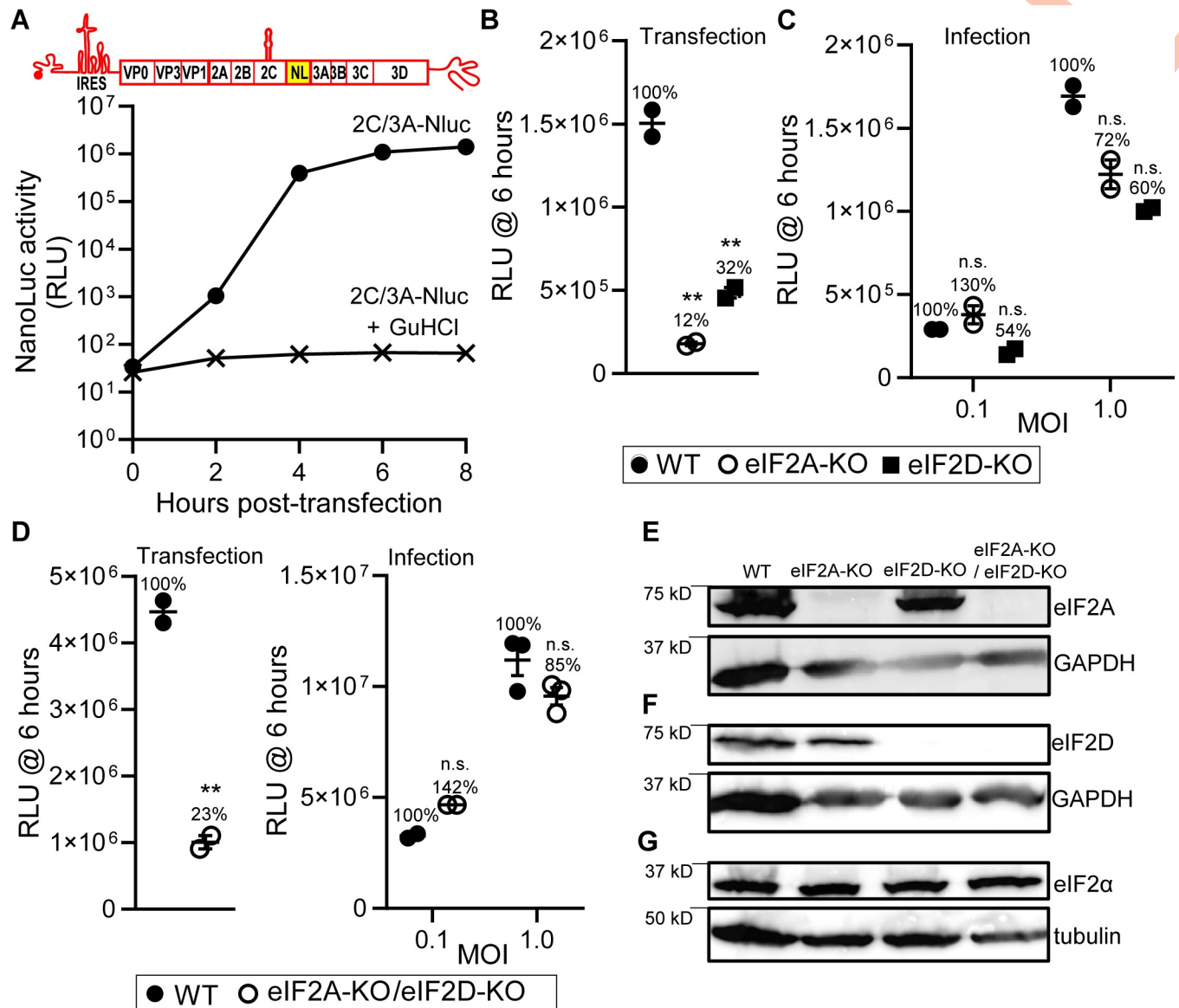
Fig 12. Contribution of eIF2A and eIF2D to translation of enteroviral RNAs. (A) NanoLuc activity in HAP1 WT cells transfected with a full-length PV genome with the nanoLuc-coding sequence embedded between 2C- and 3A-coding regions (2C/3A-Nluc). As a control, the PV 2C/3A-Nluc RNA was transfected in the presence of GuHCl. Numerical data provided as Supporting information (S1 Data). **(B)** Comparison of nanoLuc activity at six hours posttransfection using PV 2C/3A-Nluc RNA in HAP1 WT, eIF2A-KO, and eIF2D-KO cells. Data from one of two biological replicates with similar results, each with two technical replicates. Numerical data provided as Supporting information (S1 Data). **(C)** Comparison of nanoLuc activity at six hours postinfection using an MOI of 0.1 or 1 in HAP1 WT, eIF2A-KO, and eIF2D-KO cells. Data from one of two biological replicates with similar results, each with two technical replicates. Numerical data provided as Supporting information (S1 Data). **(D)** Comparison of nanoLuc activity at six hours posttransfection using PV 2C/3A-Nluc RNA (Transfection), and at six hours postinfection using an MOI of 0.1 or 1 (Infection) in HAP1 WT, and eIF2A-KO/eIF2D-KO cells. Data from one of two biological replicates with similar results, each with two or three technical replicates. Statistical analyses were performed using unpaired, two-tailed t test (** indicates $p < 0.01$, n.s. indicates not significant). Numerical data provided as Supporting information (S1 Data). **(E-G)** Western blot analysis of eIF2A (panel **E**), eIF2D (panel **F**), and eIF2α (panel **G**) in HAP1 WT, eIF2A-KO, eIF2D-KO, and eIF2A-KO/eIF2D-KO cells. Cells were processed for western blot analysis and probed using anti-eIF2A, eIF2D, and eIF2α antibodies. GAPDH and tubulin were used as a loading control for western blot. Blots provided in Supporting information (S1 Raw Images). GuHCl, guanidine hydrochloride; KO, knockout; PV, poliovirus; RLU, relative light unit; WT, wild-type.

https://doi.org/10.1371/journal.pbio.3001693.g012

Here, we applied this experimental paradigm to determine if a phenotype exists for replication of PV when eIF2A or eIF2D is not present. In the presence of eIF2A and eIF2D, PV establishes infection faster (**Fig 13A**), replicates to higher levels (**Fig 13B**), and replicates faster (**Fig**

13C) than in the absence of one of these factors. The loss of eIF2A or eIF2D essentially prevents replication of PV requiring a longer infection time (**Fig 13D**). Slow replication may occur in cells better able to use intrinsic defense to delay viral infection by activating eIF2α. The existence of two classes of cells is also supported by evaluation of the percentage of cells infected in the presence or absence of eIF2A/eIF2D. One-quarter of cells exposed to PV do not establish infection in the absence of eIF2A or eIF2D (**Fig 13E**). Quantitative analysis of the data is presented in **Fig 13F and 13G**. We conclude that the IRES-independent, eIF2A/eIF2D-dependent mechanism likely functions during normal infection when certain factors are present or not in the host cell.

Discussion

For recombination to occur between two genetically distinct genomes by a template-switching mechanism, the two genomes must be localized to the same genome-replication organelle. How enteroviral genomes are trafficked to the site of replication, however, is not known. The central hypothesis driving this study was that determinants located in the polyprotein mediated localization to the genome-replication organelle, perhaps cotranslationally (**Fig 1A and 1B**). Therefore, translation of both genomes would be a prerequisite for recombination (**Fig 1C and 1D**). Such a requirement would be consistent with previous studies by other laboratories that have established a requirement for translation of the polyprotein in *cis* for genome replication to occur [38,39]. However, we observed that inactivation of translation of a donor PV genome by deleting the IRES enhanced recombination by 5-fold over control (**Fig 2**).

Studies of several positive-strand RNA viruses, including PV, have suggested the existence of nonreplicative recombination [31,52,53]. Such a mechanism is independent of the RdRp and occurs by a direct chemical ligation of two overlapping fragments of RNA [54]. However, our studies demonstrated the requirement for an active RdRp in the IRES-deleted, donor PV genome (**Fig 3**). The dependence on an active RdRp would, by definition, indicate replicative recombination and necessitate translation by an IRES-independent mechanism. Because the IRES eliminated the entirety of the 5′-UTR, it was possible that the normal constraints on translation initiation were lost, and we were observing something cryptic and/or irrelevant [55]. We ruled out this possibility by inactivating the IRES with a 10-nt deletion; this donor PV genome also supported recombination in an RdRp-dependent manner (**Fig 4**). We reached similar conclusions using EV-A71 (**Fig 5**). Looking back at all of the studies supporting nonreplicative recombination, they all employed RNA transfection of RNAs capable of expressing the RdRp using an IRES-independent mechanism [13,31]. These previous studies never considered an alternative translation mechanism.

Together, our results suggested the compelling possibility that an IRES-independent mechanism exists for translation of the nonstructural region of the polyprotein. We were unable to detect viral proteins directly or indirectly by using standard reporters (**Fig 6**). However, we were able to exploit our previous observation that 3CD induces PI4P, even when present at levels undetectable by immunofluorescence [41]. Constructs lacking the IRES induced PI4P in a manner requiring translation through the 3C- and 3D-coding sequences (**Fig 7**). We identified an AUG codon in the 3′-end of 2A-coding sequence that is conserved among viruses comprising the enterovirus genus (**Fig 9A**). The Wimmer lab showed years ago that this region of the protein was not essential for protease function but suggested the existence of *cis*-acting replication element in this region [44]. Our reverse-genetic analysis supported the use of this AUG as the start site for IRES-independent translation (**Figs 9** and **10**).

What was unexpected, however, was that multiple, non-AUG codons also supported translation initiation (**Figs 9** and **10**). Even more unexpected was that translation initiation

E

Group	Infection %
WT	90 ± 2
eIF2A-KO	68 ± 4
eIF2D-KO	67 ± 5
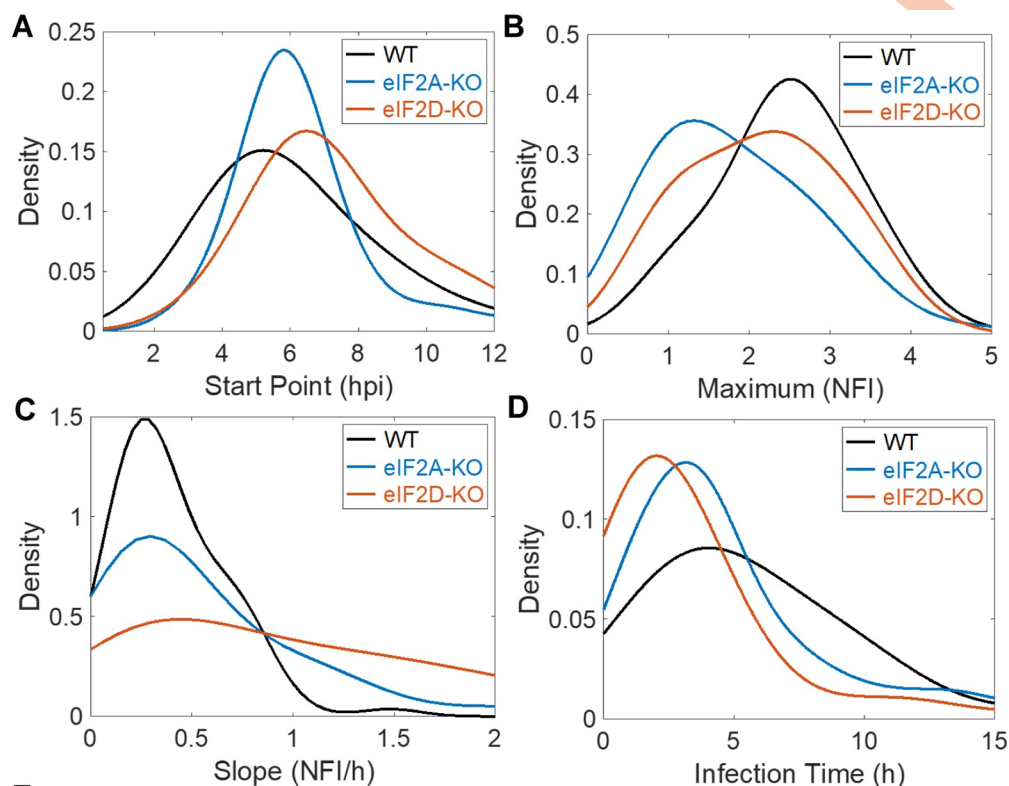
Group	WT	eIF2A-KO	eIF2D-KO
WT	1	0.0097	0.0115
eIF2A-KO	0.0097	1	0.8389
eIF2D-KO	0.0115	0.8389	1

F

Group	Cell Number	Start Point (hpi) Mean	Start Point (hpi) SD	Maximum (NFI) Mean	Maximum (NFI) SD	Slope (NFI/h) Mean	Slope (NFI/h) SD	Infection Time (h) Mean	Infection Time (h) SD
WT	173	5.01	2.31	2.21	0.93	0.38	0.31	4.09	3.16
eIF2A-KO	168	5.78	1.95	1.79	0.93	0.50	0.41	2.78	2.69
eIF2D-KO	201	6.73	2.12	2.15	0.93	0.78	0.57	3.07	2.91

G

	Group	WT	eIF2A-KO	eIF2D-KO
Start time	WT	1	0.0198	1.0105e-05
	eIF2A-KO	0.0198	1	6.0707e-04
	eIF2D-KO	1.0105e-05	6.0707e-04	1
	Group	WT	eIF2A-KO	eIF2D-KO
Maximum	WT	1	0.0012	0.6524
	eIF2A-KO	0.0012	1	0.0023
	eIF2D-KO	0.6524	0.0023	1
	Group	WT	eIF2A-KO	eIF2D-KO
Slope	WT	1	0.0386	5.2702e-07
	eIF2A-KO	0.0386	1	1.1499e-05
	eIF2D-KO	5.2702e-07	1.1499e-05	1
	Group	WT	eIF2A-KO	eIF2D-KO
Infection time	WT	1	0.0015	0.0351
	eIF2A-KO	0.0015	1	0.4266
	eIF2D-KO	0.0351	0.4266	1

Fig 13. Single-cell analysis suggests a role for eIF2A and eIF2D during infection. Single-cell analysis [50,51] using an MOI of 5 of PV-eGFP$_{PV}$ in HAP1 WT, eIF2A-KO, and eIF2D-KO cells. Comparison of the distributions of each parameter: start point (panel **A**); maximum (panel **B**); slope (panel **C**); and infection time (panel **D**); is shown (**E**) Percentage of PV-infected cells using HAP1 WT, eIF2A-KO, and eIF2D-KO cells (mean ± SD, n = 3) (Left). Adjusted P values of the t tests (Right). **(F, G)** Quantitative analysis from the data presented in panels **A**-**D**. Shown are the mean and standard deviation for each of the indicated parameters (panel **F**). Adjusted P values of the t tests (panel **G**). Numerical data provided as Supporting information (S1 Data). hpi, hours postinfection; KO, knockout; NFI, normalized fluorescence intensity; PV, poliovirus; WT, wild-type.

https://doi.org/10.1371/journal.pbio.3001693.g013

depended on eIF2A and eIF2D (**Fig 10**). These factors are essential for translation under conditions in which eIF2α has been phosphorylated, for example, in response to activation of a mediator of the integrated stress response [33]. Activation of PKR and phosphorylation of eIF2α was quite evident in our system (**Fig 8**). eIF2A and eIF2D use non-AUG codons for initiation (**Fig 10A**) [32]. However, the dependence on eIF2A and eIF2D was observed not only for a genome lacking an IRES (**Fig 10C**) but also for a genome containing an IRES (**Fig 10D**), consistent with RNA transfection activating PKR (**Fig 8**). We did not observe a strong dependence on eIF2A and/or eIF2D when infection was launched using virus (**Fig 12**).

RNA produced by in vitro transcription contains a triphosphate at the 5′-end, while the authentic viral genome would contain the 3B-encoded, genome-linked protein (VPg) [56]. In our system, cleavage by a hammerhead ribozyme leaves a hydroxyl at the 5′-end, but this modification in the context of RNA structure is known to activate PKR [57]. Fragments of the 5′-end with its triphosphate are likely not completely removed from our RNA preparations. The 5′-triphosphate is a well-known pathogen-associated molecular pattern recognized by antiviral PRRs like the double-stranded PKR [42], the interferon-inducible protein with tetratricopeptide repeats (IFIT) [58], and the retinoic acid-inducible gene product (RIG-I) [59]. Therefore, the IRES-independent, eIF2A/eIF2D-dependent mechanism of translation may have evolved to antagonize viral restriction by eIF2α kinases and IFITs.

Initiation of translation on the PV IRES uses several cellular factors [60]. eIF4G and eIF4A bind to the IRES and recruit the 43S preinitiation complex comprised of the 40S ribosomal subunit, eIF3, tRNA-Met$_i$-bound eIF2, among other factors (**Fig 14A**) [61]. We are not the first to suggest the use of an alternative translation mechanism during PV infection. The Lloyd laboratory showed that translation of the PV polyprotein late in infection does not require eIF2 [62]. The best-known eIF2-less mechanisms replace eIF2 with eIF5B [63,64] or MCT-1•DENR (multiple copies in T-cell lymphoma • density regulated protein complex) (**Fig 14B**) [65,66]. Replacement of eIF2 eliminates sensitivity to eIF2α kinases and expands the possibility for use of non-AUG codons. However, the components and mechanism for assembly of the preinitiation complex are thought to be unchanged relative to the eIF2-dependent mechanism (**Fig 14A and 14B**) [60].

Essentially, nothing is known about the eIF2A/eIF2D-dependent mechanism(s) of translation initiation in cells (**Fig 14C**) [34]. However, this mechanism is essential for cells to survive under stress and has been linked to neurodegenerative diseases and cancer [33]. Efforts to demonstrate a role for eIF2A and/or eIF2D in viral translation have been inconclusive [36,37,67,68], with the majority view being the absence of a role for either factor [67,68]. Therefore, our demonstration that enteroviruses may use these factors when intrinsic antiviral defenses have been activated may represent an opportunity not only to pursue a role for these factors in other viral systems but also to begin to define the *cis*-acting RNA determinants driving initiation of translation using these factors. In this regard, we observed a dependence of the eIF2A/eIF2D-dependent mechanism on a 78-nt *cis*-acting RNA element located upstream of the site of initiation (**Fig 11**). As discussed above, numerous mechanisms exist to function in the absence of active eIF2, so the eIF2A/eIF2D-dependent mechanism may further extend
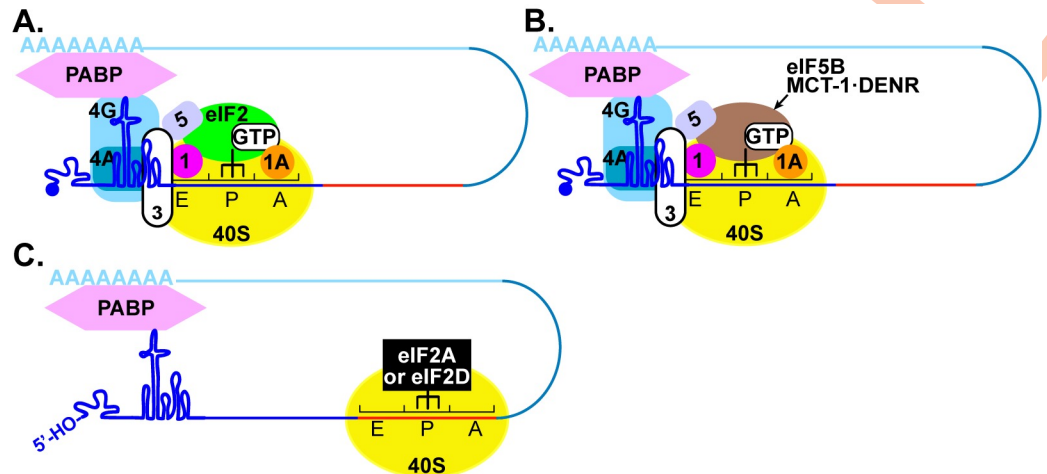
Fig 14. Models for initiation of translation on the enterovirus genome. (A) Under normal conditions, eIF4G and eIF4A bind to the primary IRES and recruit the 43S preinitiation complex composed of the 40S ribosomal subunit (yellow), eIF2/GTP/Met-tRNAi^{Met} (green), and eIF3, among other factors. Initiation may also be facilitated by interactions of the poly(rA)-binding protein, PABP, bound to the 3′-poly(rA) tail. This interaction may use eIF4G or viral/cellular factors interacting with the cloverleaf. Translation begins at the AUG start site in an eIF2-directed manner. **(B)** Multiple distinct eIF2-independent mechanisms exist. Both eIF5B and MCT-1•DENR (brown) can substitute for eIF2 to promote recruitment of initiator tRNA and translation initiation at the AUG start site. These factors may also initiate at non-AUG codons. **(C)** A canonical IRES-independent, eIF2A/eIF2D-dependent mechanism. Activation of intrinsic antiviral defense mechanisms, for example, as a result of the presence of the 5′-OH as a component of structured RNA in our biosynthetic enteroviral genomes, will lead to inactivation of eIF2 and perhaps even sequestration of eIF3. The noncanonical translation initiation factors eIF2A and eIF2D (black) direct translation initiation from a region of RNA (red) within 2A-coding sequence in a manner that is not dependent on the presence of an AUG codon but may require *cis*-acting RNA element upstream of the site of translation initiation as suggested by the studies reported herein. Other than the 40S ribosomal subunit, factors leading to formation of the translation–initiation complex are not known.

independence from canonical initiation factors. One candidate would be eIF3. IFITs activated by 5′-ppp-RNA sequester eIF3 to diminish translation. Any residual 5′-ppp fragments produced during in vitro transcription should activate IFITs. The IRES-independent, eIF2A/eIF2D-dependent mechanism would therefore be predicted to function in the absence of eIF3.

Our studies of PV infection at the population level concealed any significant difference in replication in the presence or absence of eIF2A or eIF2D (**Fig 12C and 12D**). However, studies at the single-cell level revealed a clear advantage to having both genes expressed (**Fig 13A and 13B**). There were two intriguing observations. First, infections that required longer than 5 hours for completion appeared to be lost in the absence of eIF2A or eIF2D (**Fig 13E**). This population may reflect those in which the IRES-independent, eIF2A/eIF2D-dependent mechanism was required, perhaps because the infecting PV variant activated intrinsic defenses. Second, 25% of the cells appeared recalcitrant to infection in the absence of eIF2A or eIF2D (**Fig 13E**). Perhaps intrinsic defenses are up-regulated independent of infection in this population of cells. The bottom line is that virus variant- and/or host-driven circumstances exist that require eIF2A and/or eIF2D for proper resolution, and the requirement for these factors may only become apparent by using a single-cell analysis.

The literature on eIF2A and eIF2D suggests that each functions independently of the other. This circumstance may merely reflect that each protein has been studied in the absence of the other. Our results show quite clearly that loss of eIF2A or eIF2D alone reduces translation to the same extent and causes an equivalent phenotype (**Fig 12B**), without any further reduction observed when expression of both proteins is eliminated (**Fig 12D**). These data suggest cooperation between these proteins. The stability of each is independent of the other (**Fig 12D**).

Perhaps recruitment to or function on the ribosome requires both when eIF2A/eIF2D-dependent mechanism of translation is engaged.

Group B enteroviruses establish persistent infections in the heart and pancreas that lead to myocarditis and diabetes, respectively [69,70]. Deletion of the 5′-terminal *cis*-acting replication element, the so-called cloverleaf, is a signature of the genomes that persist in the heart [71]. How these deletions impact IRES-dependent translation is unclear, but viral proteins are below the limit of detection during persistent infection [71]. The IRES-independent, eIF2A/eIF2D-dependent translation mechanism exhibits all of the features one might expect to support persistence of an enteroviral genome. Capsid proteins would not be made, so particles would not be released, leading to inflammation or immune responses. The 2A protease is quite efficient at impairing host cell functions [72], and this protein would not be made. The 3C(D) protease can also be toxic [73]. Much of the damage caused by this protein happens late in infection, so there is likely a requirement for high concentrations of the protein. None of the nonstructural proteins accumulates to detectable levels. Genomes dependent on this alternative translation mechanism replicate and recombine as demonstrated herein.

In conclusion, this study has revealed an eIF2A/eIF2D-dependent mechanism of translation initiation used by PV that may be conserved in all enteroviruses that appears to permit continued translation and genome replication under conditions in which intrinsic antiviral defenses have been activated. Discovery of the *cis*-acting determinants driving this alternative translation mechanism will further illuminate the contributions of this mechanism to viral multiplication, fitness, and pathogenesis. Finally, our identification of a *cis*-acting RNA element contributing to eIF2A/eIF2D-dependent initiation of translation may enable elucidation of the repertoire of factors and pathway used for initiation.

Materials and methods

Cells and viruses

Adherent monolayers of HeLa and L929 fibroblasts were grown in DMEM/F-12 media. Adherent monolayers of human embryonic rhabdomyosarcoma (RD) were grown in DMEM media. WT HAP1 human haploid cells and HAP1 cells KO for eIF2A (cat# HZGHC002650c001) or eIF2D (cat# HZGHC002651c012) were purchased from Horizon Discovery Group plc. All media was supplemented with 100 U/mL penicillin, 100 μg/mL streptomycin, and 10% heat-inactivated (HI) FBS. All cells were passaged in the presence of trypsin–EDTA.

WT and recombinant viruses were recovered following transfection of RNA produced in vitro (see below) from full-length cDNA or from the cell-based assay parental partners. PV type 1 (Mahoney) and EV-A71 (C2) were used throughout this study. Virus was quantified by pfu/mL. Where stated, GuHCl (Sigma) was added to growth media at 3 mM.

Plasmids, in vitro transcription, cell transfection, and virus quantification

Subgenomic PV replicon, ΔIRES, and a replication-incompetent full-length PV genomic RNA were previously described [13]. All insertions/deletions were created using either overlap extension PCR or gBlock gene fragments from IDT. Oligonucleotides used in this study can be found in **S1 Table**. The presence of the desired insertions/deletions and the absence of additional mutations were verified by DNA sequencing. 3B STOP was modified from a full-length PV genomic RNA by introducing two STOP codons (UAGUAA) after the 3B-coding sequence. ΔSLII-3 was modified from a subgenomic PV replicon by introducing a 10-nucleotide deletion (nt 185–189, nt 198–202) into the SLII-3 region of the IRES [40]. For a full-length PV genome with the nanoLuc-coding sequence embedded between 2C- and 3A-coding

regions (2C/3A-Nluc), nanoLuciferase-encoding sequence carrying a 3C protease cleavage site at its carboxyl terminus was inserted between the 2C and the 3A regions of the PV sequence. Translation occurred from the natural PV initiation codon. Proteolytic cleavage and release of nanoLuciferase occurred by normal 3C protease activity. Plasmids encoding PV genomes (full length or subgenomic) were linearized with *ApaI*. The EV-A71 C2 replicon and ΔIRES were previously described [15]. 3B STOP was modified from a previously described EV-A71 C2-MP4 infectious clone [15,74]. The EV-A71 C2 replicon and ΔIRES were linearized with *SalI*. 3B STOP was linearized with *EagI*.

All linearized cDNAs were transcribed in vitro using T7 RNA Polymerase treated with 2U DNAse Turbo (Thermo Fisher) to remove residual DNA template. The RNA transcripts were purified using RNeasy Mini Kit (Qiagen) before spectrophotometric quantification. Purified RNA in RNase-free H_2O was transfected into cells using TransMessenger (Qiagen). Virus yield was quantified by plaque assay in either HeLa (PV) or RD (EV-A71) cells. Briefly, cells and media were harvested at time points posttransfection (specified in the main text or below), subjected to three freeze–thaw cycles, and clarified. Supernatant was then used on fresh cells in 6-well plates; virus infection was allowed to continue for 30 minutes. Media was then removed, and cells were washed with PBS (pH 7.4) before a 1% (w/v) agarose-media overlay was added. Cells were incubated for either 2 to 3 days for PV or 3 to 4 days for EV-A71 and then fixed and stained with crystal violet for virus quantification.

Antibodies

Antibody for staining PI4P was purchased from Echelon Biosciences. Antibody against PV 3D was produced in Cameron lab. Mouse monoclonal anti-GAPDH antibody (10R-G109a) was purchased from Fitzgerald Industries. All secondary antibodies used for immunofluorescence were purchased from Invitrogen. Secondary antibodies for western blotting were purchased from Amersham GE Healthcare (rabbit anti-HRP) and Cell Signaling (mouse anti-HRP). Rabbit polyclonal anti-eIF2D antibody (12840-1-AP) and anti-eIF2A antibody (11233-1-AP) were purchased from Proteintech. Rabbit anti-phospho (S51)-eIF2α (9721) and rabbit anti-eIF2α (9722) were purchased from Cell Signaling Technology. Rabbit anti-phospho (T446)-PKR (32036) and rabbit anti-PKR (32506) were purchased from Abcam.

Indirect immunofluorescence

HeLa cells were fixed 6 hours posttransfection using 4% formaldehyde in PBS for 20 minutes, followed by washing in PBS and permeabilizing with 20 μM digitonin for 10 minutes. Digitonin was removed, and cells were rinsed three times with PBS. Cells were then blocked with 3% BSA in PBS for 1 hour and incubated with primary antibodies for 1 hour. Following washes, cells were incubated with secondary antibodies for 1 hour, followed by a 10-minute DAPI incubation. The processed coverslips were mounted on glass slides using ProLong Glass Anti-fade Mountant (Thermo Scientific). Samples were imaged using the Keyence BZ-X800. Primary antibodies are anti-PI4P (1:200) and anti-3D (1:100). All dilutions were made in the blocking buffer.

Western blotting

Cells were lysed in radioimmunoprecipitation assay (RIPA) buffer containing an inhibitor cocktail of phenylmethylsulfonyl fluoride (PMSF) (1:100) (American Bioanalytical), Protease Inhibitor Cocktail (Sigma-Aldrich) (1:100), and Phosphatase Inhibitor Cocktail I (Abcam) (1:100). Lysates were collected and clarified by centrifugation. The lysate was mixed with 4× Laemmli buffer, boiled, and then processed by SDS-PAGE. The samples were then transferred

from the gel to a 20-μm nitrocellulose membrane (Bio-Rad) using the TurboBlot system (Bio-Rad). Membranes were blocked in 5% dry milk with 0.1% Tween-20 or Everyday Blocking Reagent (Bio-Rad) and probed with anti-eIF2A (1:1,000), anti-eIF2D (1:1,000), anti-p-eIF2α (1:1,000), anti-p-PKR (1:1,000), anti-eIF2α (1:2,500), or anti-PKR (1:2,500) antibodies overnight. Anti-rabbit/mouse immunoglobulin G antibody coupled to peroxidase (Amersham GE Healthcare) were used as secondary antibody at a 1:5,000 dilution. Protein bands were visualized with the ECL detection system (Amersham, GE Healthcare). Where stated, membranes were subjected to reprobing against anti-tubulin (1:5,000) or anti-GAPDH (1:5,000).

Luciferase assays

Subgenomic luciferase assays were performed as described previously [25]. For each time point, 1.0×10^5 cells were suspended in 100 μl lysis buffer, and 10 μl was used for measuring luciferase activity. Considering the corresponding luciferase molecules to the limit of detection, up to 1,200 molecules (1.2×10^7 molecules/1.0×10^4 cells) of luciferase may exist in a cell transfected with RNAs containing either a deleted IRES or ΔSLII-3.

NanoLuc assays were carried out with the NLuc GLOW Assay kit (Nanolight Technology, #325) following the manufacturer's protocol.

Cell-based recombination assay

Assays were used as described previously [13–15,75]. For the cell-based assay using HAP1 cells, unless otherwise stated, equivalent ratios of RNA (total 0.5 μg) were cotransfected into HAP1 cells in 12-well dishes. Cells and media were harvested at 6 hours posttransfection, subjected to three freeze–thaw cycles, and clarified. Virus yield was quantified by plaque assay in HeLa cells.

Single-cell analysis

For each group, cells were infected with PV-eGFP$_{PV}$ at the MOI of 5 PFU per cell. On-chip experiments and data processing were done as described previously [50,51].

Supporting information

S1 Table. Oligonucleotides used in the study.
(DOCX)

S1 Data. Numerical data.
(XLSX)

S1 Raw Images. Blots.
(PDF)

Author Contributions

Conceptualization: Jamie J. Arnold, Craig E. Cameron.

Data curation: Hyejeong Kim.

Formal analysis: Hyejeong Kim, David Aponte-Diaz, Mohamad S. Sotoudegan, Djoshkun Shengjuler, Jamie J. Arnold, Craig E. Cameron.

Funding acquisition: Jamie J. Arnold, Craig E. Cameron.

Investigation: Hyejeong Kim, David Aponte-Diaz, Mohamad S. Sotoudegan, Djoshkun Shengjuler.

Methodology: Hyejeong Kim, Djoshkun Shengjuler, Craig E. Cameron.

Project administration: Jamie J. Arnold, Craig E. Cameron.

Supervision: Jamie J. Arnold, Craig E. Cameron.

Validation: Hyejeong Kim, David Aponte-Diaz, Mohamad S. Sotoudegan.

Visualization: Hyejeong Kim, David Aponte-Diaz, Mohamad S. Sotoudegan, Djoshkun Shengjuler.

Writing – original draft: Hyejeong Kim, Craig E. Cameron.

Writing – review & editing: Hyejeong Kim, David Aponte-Diaz, Mohamad S. Sotoudegan, Djoshkun Shengjuler, Jamie J. Arnold, Craig E. Cameron.

References

1. Muller HJ. The Relation of Recombination to Mutational Advance. Mutat Res. 1964; 106:2–9. https://doi.org/10.1016/0027-5107(64)90047-8 PMID: 14195748

2. Felsenstein J. The evolutionary advantage of recombination. Genetics. 1974; 78(2):737–756. https://doi.org/10.1093/genetics/78.2.737 PMID: 4448362

3. Simon-Loriere E, Holmes EC. Why do RNA viruses recombine? Nat Rev Microbiol. 2011; 9(8):617–626. https://doi.org/10.1038/nrmicro2614 PMID: 21725337

4. Cuervo NS, Guillot S, Romanenkova N, Combiescu M, Aubert-Combiescu A, Seghier M, et al. Genomic features of intertypic recombinant sabin poliovirus strains excreted by primary vaccinees. J Virol. 2001; 75(13):5740–5751. https://doi.org/10.1128/JVI.75.13.5740-5751.2001 PMID: 11390576

5. Hahn CS, Lustig S, Strauss EG, Strauss JH. Western equine encephalitis virus is a recombinant virus. Proc Natl Acad Sci U S A. 1988; 85(16):5997–6001. https://doi.org/10.1073/pnas.85.16.5997 PMID: 3413072

6. Graham RL, Baric RS. Recombination, reservoirs, and the modular spike: mechanisms of coronavirus cross-species transmission. J Virol. 2010; 84(7):3134–3146. https://doi.org/10.1128/JVI.01394-09 PMID: 19906932

7. Cannon JL, Barclay L, Collins NR, Wikswo ME, Castro CJ, Magaña LC, et al. Genetic and Epidemiologic Trends of Norovirus Outbreaks in the United States from 2013 to 2016 Demonstrated Emergence of Novel GII.4 Recombinant Viruses. J Clin Microbiol. 2017; 55(7):2208–2221. https://doi.org/10.1128/JCM.00455-17 PMID: 28490488

8. Amoutzias GD, Nikolaidis M, Tryfonopoulou E, Chlichlia K, Markoulatos P, Oliver SG. The Remarkable Evolutionary Plasticity of Coronaviruses by Mutation and Recombination: Insights for the COVID-19 Pandemic and the Future Evolutionary Paths of SARS-CoV-2. Viruses. 2022; 14(1):78. https://doi.org/10.3390/v14010078 PMID: 35062282

9. Kew O, Morris-Glasgow V, Landaverde M, Burns C, Shaw J, Garib Z, et al. Outbreak of poliomyelitis in Hispaniola associated with circulating type 1 vaccine-derived poliovirus. Science. 2002; 296 (5566):356–359. https://doi.org/10.1126/science.1068284 PMID: 11896235

10. Kirkegaard K, Baltimore D. The mechanism of RNA recombination in poliovirus. Cell. 1986; 47(3):433–443. https://doi.org/10.1016/0092-8674(86)90600-8 PMID: 3021340

11. Copper PD, Steiner-Pryor A, Scotti PD, Delong D. On the nature of poliovirus genetic recombinants. J Gen Virol. 1974; 23(1):41–49. https://doi.org/10.1099/0022-1317-23-1-41 PMID: 4364875

12. Sergiescu D, Aubert-Combiescu A, Crainic R. Recombination between guanidine-resistant and dextran sulfate-resistant mutants of type 1 poliovirus. J Virol. 1969; 3(3):326–330. https://doi.org/10.1128/JVI.3.3.326-330.1969 PMID: 4305674

13. Lowry K, Woodman A, Cook J, Evans DJ. Recombination in enteroviruses is a biphasic replicative process involving the generation of greater-than genome length 'imprecise' intermediates. PLoS Pathog. 2014; 10(6):e1004191. https://doi.org/10.1371/journal.ppat.1004191 PMID: 24945141

14. Woodman A, Arnold JJ, Cameron CE, Evans DJ. Biochemical and genetic analysis of the role of the viral polymerase in enterovirus recombination. Nucleic Acids Res. 2016; 44(14):6883–6895. https://doi.org/10.1093/nar/gkw567 PMID: 27317698

15. Woodman A, Lee KM, Janissen R, Gong YN, Dekker NH, Shih SR, et al. Predicting Intraserotypic Recombination in Enterovirus 71. J Virol. 2019; 93(4):e02057–02018. https://doi.org/10.1128/JVI.02057-18 PMID: 30487277

16. Li C, Wang H, Shi J, Yang D, Zhou G, Chang J, et al. Senecavirus-Specific Recombination Assays Reveal the Intimate Link between Polymerase Fidelity and RNA Recombination. J Virol. 2019; 93(13):e00576–00519. https://doi.org/10.1128/JVI.00576-19 PMID: 30996084

17. Arnold JJ, Cameron CE. Poliovirus RNA-dependent RNA polymerase (3Dpol) is sufficient for template switching in vitro. J Biol Chem. 1999; 274(5):2706–2716. https://doi.org/10.1074/jbc.274.5.2706 PMID: 9915801

18. Xiao Y, Rouzine IM, Bianco S, Acevedo A, Goldstein EF, Farkov M, et al. RNA Recombination Enhances Adaptability and Is Required for Virus Spread and Virulence. Cell Host Microbe. 2016; 19(4):493–503. https://doi.org/10.1016/j.chom.2016.03.009 PMID: 27078068

19. Janissen R, Woodman A, Shengjuler D, Vallet T, Lee KM, Kuijpers L, et al. Induced intra- and intermolecular template switching as a therapeutic mechanism against RNA viruses. Mol Cell. 2021; 81(21):4467–80.e7. https://doi.org/10.1016/j.molcel.2021.10.003 PMID: 34687604

20. Dulin D, Arnold JJ, van Laar T, Oh HS, Lee C, Perkins AL, et al. Signatures of Nucleotide Analog Incorporation by an RNA-Dependent RNA Polymerase Revealed Using High-Throughput Magnetic Tweezers. Cell Rep. 2017; 21(4):1063–1076. https://doi.org/10.1016/j.celrep.2017.10.005 PMID: 29069588

21. Altan-Bonnet N. Lipid Tales of Viral Replication and Transmission. Trends Cell Biol. 2017; 27(3):201–213. https://doi.org/10.1016/j.tcb.2016.09.011 PMID: 27838086

22. Dahmane S, Kerviel A, Morado DR, Shankar K, Ahlman B, Lazarou M, et al. Membrane-assisted assembly and selective secretory autophagy of enteroviruses. Nat Commun. 2022; 13(1):5986. https://doi.org/10.1038/s41467-022-33483-7 PMID: 36216808

23. Hsu NY, Ilnytska O, Belov G, Santiana M, Chen YH, Takvorian PM, et al. Viral reorganization of the secretory pathway generates distinct organelles for RNA replication. Cell. 2010; 141(5):799–811. https://doi.org/10.1016/j.cell.2010.03.050 PMID: 20510927

24. Jackson WT. Poliovirus-induced changes in cellular membranes throughout infection. Curr Opin Virol. 2014; 9:67–73. https://doi.org/10.1016/j.coviro.2014.09.007 PMID: 25310497

25. Oh HS, Banerjee S, Aponte-Diaz D, Sharma SD, Aligo J, Lodeiro MF, et al. Multiple poliovirus-induced organelles suggested by comparison of spatiotemporal dynamics of membranous structures and phosphoinositides. PLoS Pathog. 2018; 14(4):e1007036. https://doi.org/10.1371/journal.ppat.1007036 PMID: 29702686

26. Dorner AJ, Dorner LF, Larsen GR, Wimmer E, Anderson CW. Identification of the initiation site of poliovirus polyprotein synthesis. J Virol. 1982; 42(3):1017–1028. https://doi.org/10.1128/JVI.42.3.1017-1028.1982 PMID: 6284987

27. Pelletier J, Sonenberg N. Internal initiation of translation of eukaryotic mRNA directed by a sequence derived from poliovirus RNA. Nature. 1988; 334(6180):320–325. https://doi.org/10.1038/334320a0 PMID: 2839775

28. Trono D, Pelletier J, Sonenberg N, Baltimore D. Translation in mammalian cells of a gene linked to the poliovirus 5′ noncoding region. Science. 1988; 241(4864):445–448. https://doi.org/10.1126/science.2839901 PMID: 2839901

29. Jang SK, Davies MV, Kaufman RJ, Wimmer E. Initiation of protein synthesis by internal entry of ribosomes into the 5′ nontranslated region of encephalomyocarditis virus RNA in vivo. J Virol. 1989; 63(4):1651–1660. https://doi.org/10.1128/JVI.63.4.1651-1660.1989 PMID: 2538648

30. Pilipenko EV, Gmyl AP, Maslova SV, Svitkin YV, Sinyakov AN, Agol VI. Prokaryotic-like cis elements in the cap-independent internal initiation of translation on picornavirus RNA. Cell. 1992; 68(1):119–131. https://doi.org/10.1016/0092-8674(92)90211-t PMID: 1310072

31. Gmyl AP, Belousov EV, Maslova SV, Khitrina EV, Chetverin AB, Agol VI. Nonreplicative RNA recombination in poliovirus. J Virol. 1999; 73(11):8958–8965. https://doi.org/10.1128/JVI.73.11.8958-8965.1999 PMID: 10516001

32. Kearse MG, Wilusz JE. Non-AUG translation: a new start for protein synthesis in eukaryotes. Genes Dev. 2017; 31(17):1717–1731. https://doi.org/10.1101/gad.305250.117 PMID: 28982758

33. Green KM, Miller SL, Malik I, Todd PK. Non-canonical initiation factors modulate repeat-associated non-AUG translation. Hum Mol Genet. 2022; 31(15):2521–2534. https://doi.org/10.1093/hmg/ddac021 PMID: 35220421

34. Komar AA, Merrick WC. A Retrospective on eIF2A-and Not the Alpha Subunit of eIF2. Int J Mol Sci. 2020; 21(6):2054. https://doi.org/10.3390/ijms21062054 PMID: 32192132

35. Wek RC. Role of eIF2alpha Kinases in Translational Control and Adaptation to Cellular Stress. Cold Spring Harb Perspect Biol. 2018; 10(7):a032870.

36. Sanz MA, Gonzalez Almela E, Carrasco L. Translation of Sindbis Subgenomic mRNA is Independent of eIF2, eIF2A and eIF2D. Sci Rep. 2017; 7:43876. https://doi.org/10.1038/srep43876 PMID: 28240315

37. Gonzalez-Almela E, Williams H, Sanz MA, Carrasco L. The Initiation Factors eIF2, eIF2A, eIF2D, eIF4A, and eIF4G Are Not Involved in Translation Driven by Hepatitis C Virus IRES in Human Cells. Front Microbiol. 2018; 9:207. https://doi.org/10.3389/fmicb.2018.00207 PMID: 29487587

38. Novak JE, Kirkegaard K. Coupling between genome translation and replication in an RNA virus. Genes Dev. 1994; 8(14):1726–1737. https://doi.org/10.1101/gad.8.14.1726 PMID: 7958852

39. Egger D, Teterina N, Ehrenfeld E, Bienz K. Formation of the poliovirus replication complex requires coupled viral translation, vesicle production, and viral RNA synthesis. J Virol. 2000; 74(14):6570–6580. https://doi.org/10.1128/jvi.74.14.6570-6580.2000 PMID: 10864671

40. Ishii T, Shiroki K, Iwai A, Nomoto A. Identification of a new element for RNA replication within the internal ribosome entry site of poliovirus RNA. J Gen Virol. 1999; 80(Pt 4):917–920. https://doi.org/10.1099/0022-1317-80-4-917 PMID: 10211960

41. Banerjee S, Aponte-Diaz D, Yeager C, Sharma SD, Ning G, Oh HS, et al. Hijacking of multiple phospholipid biosynthetic pathways and induction of membrane biogenesis by a picornaviral 3CD protein. PLoS Pathog. 2018; 14(5):e1007086. https://doi.org/10.1371/journal.ppat.1007086 PMID: 29782554

42. Nallagatla SR, Hwang J, Toroney R, Zheng X, Cameron CE, Bevilacqua PC. 5′-triphosphate-dependent activation of PKR by RNAs with short stem-loops. Science. 2007; 318(5855):1455–1458. https://doi.org/10.1126/science.1147347 PMID: 18048689

43. Sweeney TR, Abaeva IS, Pestova TV, Hellen CU. The mechanism of translation initiation on Type 1 picornavirus IRESs. EMBO J. 2014; 33(1):76–92. https://doi.org/10.1002/embj.201386124 PMID: 24357634

44. Li X, Lu HH, Mueller S, Wimmer E. The C-terminal residues of poliovirus proteinase 2A(pro) are critical for viral RNA replication but not for cis- or trans-proteolytic cleavage. J Gen Virol. 2001; 82(Pt 2):397–408. https://doi.org/10.1099/0022-1317-82-2-397 PMID: 11161279

45. Ichihara K, Matsumoto A, Nishida H, Kito Y, Shimizu H, Shichino Y, et al. Combinatorial analysis of translation dynamics reveals eIF2 dependence of translation initiation at near-cognate codons. Nucleic Acids Res. 2021; 49(13):7298–7317. https://doi.org/10.1093/nar/gkab549 PMID: 34226921

46. Kotecki M, Reddy PS, Cochran BH. Isolation and characterization of a near-haploid human cell line. Exp Cell Res. 1999; 252(2):273–280. https://doi.org/10.1006/excr.1999.4656 PMID: 10527618

47. Carette JE, Guimaraes CP, Varadarajan M, Park AS, Wuethrich I, Godarova A, et al. Haploid genetic screens in human cells identify host factors used by pathogens. Science. 2009; 326(5957):1231–1235. https://doi.org/10.1126/science.1178955 PMID: 19965467

48. HAP1 knockout cell lines Available from: https://horizondiscovery.com/en/engineered-cell-lines/products/human-hap1-knockout-cell-lines [

49. Rehwinkel J, Reis e Sousa C. Targeting the viral Achilles' heel: recognition of 5′-triphosphate RNA in innate anti-viral defence. Curr Opin Microbiol. 2013; 16(4):485–492. https://doi.org/10.1016/j.mib.2013.04.009 PMID: 23707340

50. Guo F, Li S, Caglar MU, Mao Z, Liu W, Woodman A, et al. Single-Cell Virology: On-Chip Investigation of Viral Infection Dynamics. Cell Rep. 2017; 21(6):1692–1704. https://doi.org/10.1016/j.celrep.2017.10.051 PMID: 29117571

51. Liu W, Caglar MU, Mao Z, Woodman A, Arnold JJ, Wilke CO, et al. More than efficacy revealed by single-cell analysis of antiviral therapeutics. Sci Adv. 2019; 5(10):eaax4761. https://doi.org/10.1126/sciadv.aax4761 PMID: 31692968

52. Gallei A, Pankraz A, Thiel HJ, Becher P. RNA recombination in vivo in the absence of viral replication. J Virol. 2004; 78(12):6271–6281. https://doi.org/10.1128/JVI.78.12.6271-6281.2004 PMID: 15163720

53. Kleine Büning M, Meyer D, Austermann-Busch S, Roman-Sosa G, Rümenapf T, Becher P. Nonreplicative RNA Recombination of an Animal Plus-Strand RNA Virus in the Absence of Efficient Translation of Viral Proteins. Genome Biol Evol. 2017; 9(4):817–829. https://doi.org/10.1093/gbe/evx046 PMID: 28338950

54. Chetverin AB, Chetverina HV, Demidenko AA, Ugarov VI. Nonhomologous RNA recombination in a cell-free system: evidence for a transesterification mechanism guided by secondary structure. Cell. 1997; 88(4):503–513. https://doi.org/10.1016/s0092-8674(00)81890-5 PMID: 9038341

55. Murray KE, Steil BP, Roberts AW, Barton DJ. Replication of poliovirus RNA with complete internal ribosome entry site deletions. J Virol. 2004; 78(3):1393–1402. https://doi.org/10.1128/jvi.78.3.1393-1402.2004 PMID: 14722294

56. Wimmer E, Nomoto A. Molecular biology and cell-free synthesis of poliovirus. Biologicals. 1993; 21(4):349–356. https://doi.org/10.1006/biol.1993.1095 PMID: 8024750

57. Herold J, Andino R. Poliovirus requires a precise 5′ end for efficient positive-strand RNA synthesis. J Virol. 2000; 74(14):6394–6400. https://doi.org/10.1128/jvi.74.14.6394-6400.2000 PMID: 10864650

58. Pichlmair A, Lassnig C, Eberle CA, Górna MW, Baumann CL, Burkard TR, et al. IFIT1 is an antiviral protein that recognizes 5′-triphosphate RNA. Nat Immunol. 2011; 12(7):624–630. https://doi.org/10.1038/ni.2048 PMID: 21642987

59. Hornung V, Ellegast J, Kim S, Brzózka K, Jung A, Kato H, et al. 5′-Triphosphate RNA is the ligand for RIG-I. Science. 2006; 314(5801):994–997. https://doi.org/10.1126/science.1132505 PMID: 17038590

60. Komar AA, Mazumder B, Merrick WC. A new framework for understanding IRES-mediated translation. Gene. 2012; 502(2):75–86. https://doi.org/10.1016/j.gene.2012.04.039 PMID: 22555019

61. Martinez-Salas E, Pacheco A, Serrano P, Fernandez N. New insights into internal ribosome entry site elements relevant for viral gene expression. J Gen Virol. 2008; 89(Pt 3):611–626. https://doi.org/10.1099/vir.0.83426-0 PMID: 18272751

62. White JP, Reineke LC, Lloyd RE. Poliovirus switches to an eIF2-independent mode of translation during infection. J Virol. 2011; 85(17):8884–8893. https://doi.org/10.1128/JVI.00792-11 PMID: 21697471

63. Choi SK, Lee JH, Zoll WL, Merrick WC, Dever TE. Promotion of met-tRNAiMet binding to ribosomes by yIF2, a bacterial IF2 homolog in yeast. Science. 1998; 280(5370):1757–1760. https://doi.org/10.1126/science.280.5370.1757 PMID: 9624054

64. Pestova TV, de Breyne S, Pisarev AV, Abaeva IS, Hellen CU. eIF2-dependent and eIF2-independent modes of initiation on the CSFV IRES: a common role of domain II. EMBO J. 2008; 27(7):1060–1072. https://doi.org/10.1038/emboj.2008.49 PMID: 18337746

65. Dmitriev SE, Terenin IM, Andreev DE, Ivanov PA, Dunaevsky JE, Merrick WC, et al. GTP-independent tRNA delivery to the ribosomal P-site by a novel eukaryotic translation factor. J Biol Chem. 2010; 285(35):26779–26787. https://doi.org/10.1074/jbc.M110.119693 PMID: 20566627

66. Skabkin MA, Skabkina OV, Dhote V, Komar AA, Hellen CU, Pestova TV. Activities of Ligatin and MCT-1/DENR in eukaryotic translation initiation and ribosomal recycling. Genes Dev. 2010; 24(16):1787–1801. https://doi.org/10.1101/gad.1957510 PMID: 20713520

67. Ventoso I, Sanz MA, Molina S, Berlanga JJ, Carrasco L, Esteban M. Translational resistance of late alphavirus mRNA to eIF2alpha phosphorylation: a strategy to overcome the antiviral effect of protein kinase PKR. Genes Dev. 2006; 20(1):87–100. https://doi.org/10.1101/gad.357006 PMID: 16391235

68. Kim JH, Park SM, Park JH, Keum SJ, Jang SK. eIF2A mediates translation of hepatitis C viral mRNA under stress conditions. EMBO J. 2011; 30(12):2454–2464. https://doi.org/10.1038/emboj.2011.146 PMID: 21556050

69. Lloyd RE, Tamhankar M, Lernmark Å. Enteroviruses and Type 1 Diabetes: Multiple Mechanisms and Factors? Annu Rev Med. 2022; 73:483–499. https://doi.org/10.1146/annurev-med-042320-015952 PMID: 34794324

70. Kim KS, Hufnagel G, Chapman NM, Tracy S. The group B coxsackieviruses and myocarditis. Rev Med Virol. 2001; 11(6):355–368. https://doi.org/10.1002/rmv.326 PMID: 11746998

71. Bouin A, Gretteau PA, Wehbe M, Renois F, N'Guyen Y, Leveque N, et al. Enterovirus Persistence in Cardiac Cells of Patients With Idiopathic Dilated Cardiomyopathy Is Linked to 5' Terminal Genomic RNA-Deleted Viral Populations With Viral-Encoded Proteinase Activities. Circulation. 2019; 139(20):2326–2338. https://doi.org/10.1161/CIRCULATIONAHA.118.035966 PMID: 30755025

72. Castelló A, Alvarez E, Carrasco L. The multifaceted poliovirus 2A protease: regulation of gene expression by picornavirus proteases. J Biomed Biotechnol. 2011; 2011:369648. https://doi.org/10.1155/2011/369648 PMID: 21541224

73. Sun D, Chen S, Cheng A, Wang M. Roles of the Picornaviral 3C Proteinase in the Viral Life Cycle and Host Cells. Viruses. 2016; 8(3):82. https://doi.org/10.3390/v8030082 PMID: 26999188

74. Wang YF, Chou CT, Lei HY, Liu CC, Wang SM, Yan JJ, et al. A mouse-adapted enterovirus 71 strain causes neurological disease in mice after oral infection. J Virol. 2004; 78(15):7916–7924. https://doi.org/10.1128/JVI.78.15.7916-7924.2004 PMID: 15254164

75. Kim H, Ellis VD 3rd, Woodman A, Zhao Y, Arnold JJ, Cameron CE. RNA-Dependent RNA Polymerase Speed and Fidelity are not the Only Determinants of the Mechanism or Efficiency of Recombination. Genes (Basel). 2019; 10(12):968. https://doi.org/10.3390/genes10120968 PMID: 31775299